used in combination with IFN-α to ameliorate the salvage rate of HCV infection [2]. It is necessary to improve the salvage rate of HCV infection by clarifying the efficacy of IFN treatment since IFN-α is the most basic agent for HCV treatment. Any agents that can support IFN activity will improve the therapeutic effect for HCV infected patients.

Geranylgeranylacetone (GGA), an isoprenoid compound, which includes retinoids, has been used orally as an anti-ulcer drug developed in Japan [3]. GGA protects the gastric mucosa from various types of stress without affecting gastric acid secretion [4, 5]. Moreover, GGA suppresses cell growth and induces differentiation or apoptosis in several human leukemia cells [6, 7]. Another isoprenoid compound, 3,7,11,15-tetramethyl-2,4,6,-10,14-hexadecapentaenoic acid, which is designated as an acyclic retinoid because it has the ability to interact with nuclear retinoid receptors [8], causes apoptosis in certain human hepatoma cells [9]. GGA acts as a potent inducer of antiviral gene expression by stimulating the ISGF3 formation in human hepatoma cells [10]. GGA induces the expression of antiviral proteins such as 2′5′-oligoadenylate synthetase (2′5′-OAS) and double-stranded RNA-dependent protein kinase (PKR) in hepatoma cell lines. GGA stimulates 2′5′-OAS and PKR gene expression at the transcriptional level through the formation of interferon-stimulated gene factor 3 (ISGF-3), which regulates the transcription of both genes. GGA induces the expression of signal transducers and activators of transcription 1, 2 (STAT-1, STAT-2) and p48 proteins, components of ISGF3, together with the phosphorylation of STAT1 [10]. However, no anti-HCV activity was observed.

A cell culture HCV replicon system has been developed as a useful tool for the study of HCV replication and mass screening for anti-HCV reagents. OR6 cells stably harboring the full-length genotype 1 replicon containing the *Renilla* luciferase gene, ORN/C-5B/KE [11], were used to examine the influence of the anti-HCV effect of IFN. The luciferase activity in cell lysate of OR6 was correlated with the HCV-RNA concentration, and the IC50 of IFN-α was less than 10 IU/mL [11]. The OR6 system is a useful and sensitive cell culture replicon system.

This study verified the anti-HCV activity of GGA in the OR6 system. In addition, the mechanisms of anti-HCV activity were examined in OR6 cells.

Materials and methods

Reagents

GGA was a generous gift from Eisai Co. (Tokyo, Japan). Recombinant human IFN-α2a was purchased from Nippon Roche Co. (Tokyo, Japan). Wortmannin, LY294002, Akt inhibitor and rapamycin were purchased from Calbiochem (La Jolla, CA, USA).

HCV replicon system

OR6 cells stably harboring the full-length genotype 1 replicon, ORN/C-5B/KE, were used to examine the influence of the anti-HCV effect of GGA. The cells were cultured in Dulbecco's modified Eagle's medium (Gibco-BRL, Invitrogen) supplemented with 10% fatal bovine serum, penicillin and streptomycin and maintained in the presence of G418 (300 mg/L; Geneticin, Invitrogen). This replicon was derived from the 1B-2 strain (strain HCV-o, genotype 1b), in which the *Renilla* luciferase gene is introduced as a fusion protein with neomycin to facilitate the monitoring of HCV replication.

Reporter gene assay

The OR6 cells were grown in 24-well plates. One day later, the cells were incubated in the absence or presence of varying concentrations of chemical blockers and GGA. After treatment, the cells were harvested with Renilla lysis reagent (Promega, Madison, WI, USA) and luciferase activity in the cells was determined using a luciferase reporter assay system and a TD-20/20 luminometer. The data were expressed as the relative luciferase activity.

Western blotting and antibodies

Western blotting with anti-STAT-1, anti-PKR (Santa Cruz Biotechnology, Santa Cruz, CA, USA), anti-tyrosine-701 phosphorylated STAT-1, anti-serine-727 phosphorylated STAT-1, anti-serine-2448 phosphorylated mTOR, anti-mTOR, anti-threonine-389 phosphorylated p70S6K, anti-p70S6K (Cell Signaling, Beverly, MA, USA) and anti-HSP70 (Stressmarq Biosciences Inc, Victoria, Canada) was performed as described previously [10]. Briefly, OR6 cells were lysed by the addition of a lysis buffer (50 mmol/L Tris–HCl, pH 7.4, 1% Np40, 0.25% sodium deoxycholate, 0.02% sodium azide, 0.1% SDS, 150 mmol/L NaCl, 1 mmol/L EDTA, 1 mmol/L PMSF, 1 mg/mL each of aprotinin, leupeptin and pepstatin, 1 mmol/L sodium *o*-vanadate and 1 mmol/L NaF). The samples were separated by electrophoresis on 8–12% SDS polyacrylamide gels and electrotransferred to nitrocellulose membranes, and then blotted with each antibody. The membranes were incubated with horseradish peroxidase-conjugated anti-rabbit IgG or anti-mouse IgG, and the immunoreactive bands were visualized using the ECL chemiluminescence system (Amersham Life Science, Buckinghamshire, England).

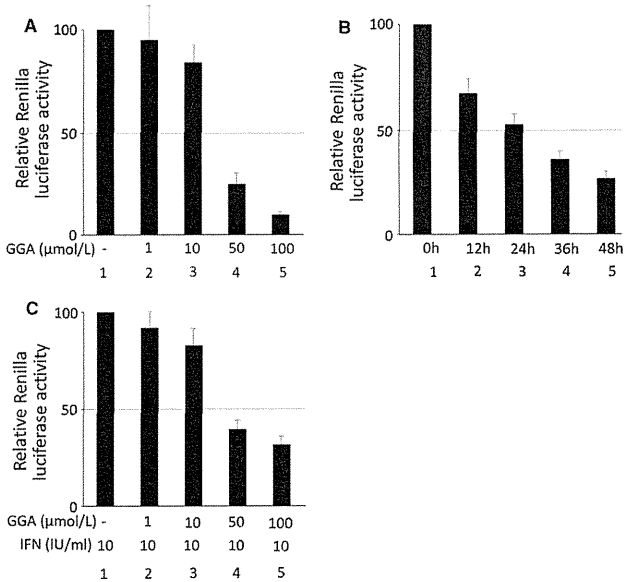

Fig. 1 The effect of GGA on the genome-length HCV RNA replication system. **a** Dose dependent effect of GGA. **b** Time course of GGA suppressed HCV replication. **c** The additive effect of GGA with IFN-α suppressed HCV replication. **a** The OR6 cells were treated with 1–100 μmol/L of GGA (*lanes 2–5*) and *lane 1* was not treated. One day later, *Renilla* luciferase activity was determined by luminometer ($n = 4$). The data are expressed as the mean ± SD and are representative of four similar experiments. The differences between *lane 3* versus *4*, *lane 3* versus *5* and *lane 3* versus *5* were statistically significant. **b** The OR6 cells were treated 50 μmol/L of GGA and at the indicated time, HCV replicon assay was done ($n = 4$). The differences between *lane 1* versus *3–5* and *lane 2* versus *4*, *5* were statistically significant. **c** The OR6 cells were treated with 10 IU/mL of IFN-α in the absence (*lane 1*) or presence of treatment with 1–100 μmol/L of GGA (*lanes 2–5*). Non-treatment OR6 cells has 100% of relative *Renilla* luciferase light unit. The differences between *lane 1* versus *4*, *5* were statistically significant. Statistical significance was accepted as a P value of <0.05. The data are expressed as the mean ± SD and are representative of four similar experiments

siRNA transfection assay

mTOR gene knockdown was performed using siRNA (Cell Signaling, Beverly, MA, USA). OR6 cells were transfected with100 nmol/L mTOR specific and non-targeted siRNA as a control in accordance with the appended manual. One day later, the cells were incubated in either the absence or presence of 50 μmol/L GGA.

mTOR kinase activity assay

The cells were washed two times with TBS and lysed by addition of lysis buffer [50 mM Tris HCl, pH 7.4, 100 mM NaCl, 50 mM β-glycerophosphate, 10% glycerol (w/v), 1% Tween-20 detergent (w/v), 1 mM EDTA, 20 nM microcystin-LR, 25 mM NaF, and a cocktail of protease inhibitors]. The insoluble materials were removed by centrifugation at 10,000 rpm for 15 min at 4°C, and the supernatants were collected and subjected to analysis of the mTOR kinase activity using a commercially available kit (Calbiochem, San Diego, USA) according to the manufacturer's instructions.

Results

GGA with or without IFN had anti-HCV activity

OR6 cells, the full-length HCV replication system, were used to examine the effect of GGA. The cells were treated with 1–100 μmol/L of GGA for 24 h and the amount of HCV replicon was measured by the *Renilla* luciferase assay (Fig. 1a). The relative *Renilla* luciferase activity decreased in a dose-dependent manner. Furthermore, GGA

induced anti-HCV replicon activity was time dependent (Fig. 1b). GGA was combined with IFN-α to examine the additive effect (Fig. 1c). One or 10 μmol/L of GGA combined with IFN-α decreased the relative *Renilla* luciferase activity slightly (Fig. 1c). However, 50 or 100 μmol/L of GGA combined with IFN-α decreased the relative *Renilla* luciferase activity with statistical difference. GGA treatment did not have any statistically significant effect on cell viability from 1 to 100 μmol/L of GGA for 24 h (data not shown).

GGA did not activate the tyrosine-701 and serine-727 on STAT-1, and did not induce PKR and HSP-70 in OR6 cells

GGA mediated phosphorylation of STAT-1 at the tyrosine-701 and serine-727 residues was investigated using antibodies to phospho-specific STAT-1 on OR6 cells. No phosphorylation of tyrosine-701 and serine-727 on STAT-1 was detected in OR6 cells (Fig. 2a). IFN induce anti-viral protein, PKR, and STAT-1 has an interferon stimulating responsive element (ISRE) in the promoter region [12]. The expression levels of both proteins did not change throughout this study, as indicated by a Western blotting analysis (Fig. 2b, c). Next, the role of HSP in the mechanism of GGA activity was examined because GGA is an inducer of HSP. The HSP-70 expression was increased by pre-exposure to heat shock (Fig. 2d, lanes 2, 4), but it did not increase due to the effects of GGA (Fig. 2d, lanes 3, 4).

Rapamycin and mTOR specific siRNA, but not PI3-K inhibitor and Akt inhibitor, were able to cancel the GGA induced anti-HCV activity

The role of the PI3-K-Akt-mTOR pathway the anti-HCV activity of GGA was examined in OR6 cells. The cells were treated with GGA after 3 h in the presence or absence of rapamycin as an mTOR inhibitor, Akt inhibitor, or wortmannin as a PI3-K inhibitor (Fig. 3). Pretreatment with rapamycin attenuated the anti-HCV replication effect

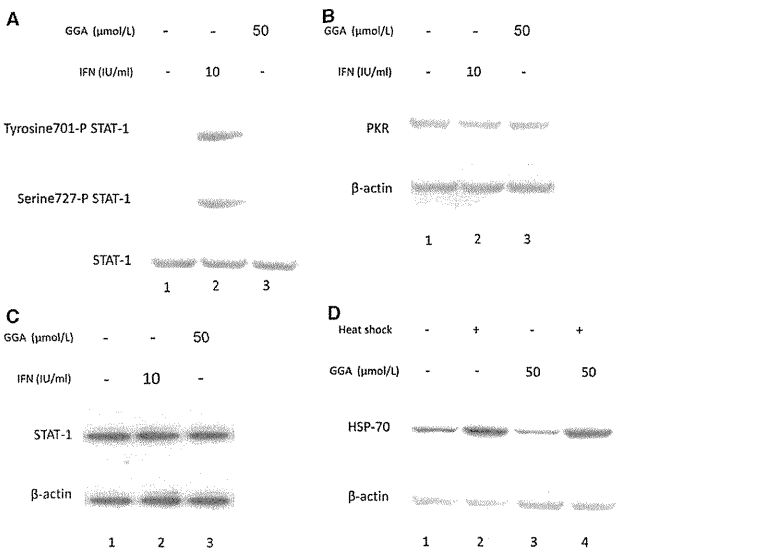

Fig. 2 Effect of GGA on STAT-1 (**a**), PKR (**b**) and HSP-70 (**c**). **a** The OR6 cells were either untreated (*lane 1*) or treated with 10 IU/mL of IFN-α (*lane 2*) for 30 min or treated with 50 μmol/L GGA (*lane 3*) and then were phosphorylated STAT-1 at tyrosine-701 residue (*upper panel*) and at serine-727 residue (*middle panel*), the expression STAT-1 (*lower panel*) was analyzed by Western blotting. **b** The OR6 cells were either untreated (*lane 1*) or treated with 10 IU/mL of IFN-α (*lane 2*) for 30 min or treated with 50 μmol/L GGA (*lane 3*), and then the expression of PKR (*upper panel*) was analyzed by a Western blotting analysis. The β-actin (*lower panel*) protein expression was used as an internal control. **c** The OR6 cells were either untreated (*lane 1*) or given heat shock (at 42°C 15 min, overnight recovery at 37°C) (*lanes 2, 4*) or treated with 50 μmol/L of GGA (*lanes 3, 4*) and then the expression HSP-70 (*upper panel*) was analyzed by Western blotting. β-Actin (*lower panel*) protein is the internal control

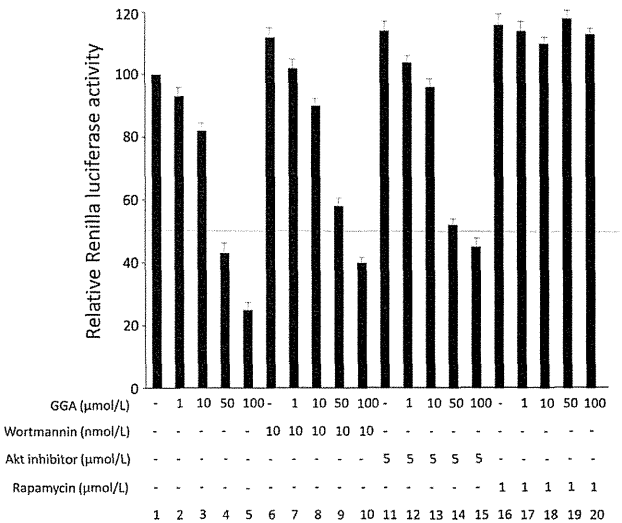

Fig. 3 Changes in GGA suppressed HCV replication by rapamycin, but not PI3-K inhibitor and Akt inhibitor. OR6 cells were treated with 1–100 μmol/L of GGA in the absence (*lanes 2–5*) or presence of pretreatment (*lanes 7–10, 12–15, 17–20*) for 3 h. *Lanes 1, 6, 11* and *16* were not treated with GGA. *Lanes 6, 11* and *16* were treated with wortmannin, an Akt inhibitor, and rapamycin, respectively. One day later, *Renilla* luciferase activity was determined by luminometer ($n = 4$). The data are expressed as the mean ± SD and are representative of four similar experiments

in comparison to GGA alone (Fig. 3, lanes 17–20), whereas pretreatment with wortmannin and Akt inhibitor did not increase the *Renilla* luciferase activity (Fig. 3, lanes 7–10, 12–15). siRNA transfection was used for mTOR knockdown to explore role of mTOR in the anti-HCV activity (Fig. 4). The transfection efficiency of the siRNA was confirmed by a Western blotting analysis. In this experiment, the detectable band intensities were quantified by the National Institutes of Health image software program. Although the transfection efficiency of siRNA was barely 46% (Fig. 4a), GGA-induced anti-HCV activity was clearly inhibited in mTOR-siRNA transfected cells (Fig. 4b, lane 4, 6) in comparison to the control cells (Fig. 4b, lanes 3, 5).

GGA induced mTOR activity, mTOR phosphorylation and p70S6K phosphorylation in OR6 cells

The phosphorylation of the serine-2448 residues of mTOR by 50 μmol/L of GGA was detected 30 min after GGA treatment. The band intensity of serine-2448 phosphorylated mTOR decreased by pretreatment with rapamycin but was almost same as with GGA alone following pretreatment with LY294002 (Fig. 5a). Furthermore, an mTOR activity assay was conducted to confirm the activity mechanism of GGA (Fig. 5b). The mTOR activity was increased by treatment with GGA alone (Fig. 5b, lane 4) and was inhibited by pretreatment with rapamycin (Fig. 5b, lane 6), whereas pretreatment with LY94002 did not suppress the mTOR activity (Fig. 5b, lane 5). Furthermore, to evaluate the mTOR activity, we investigated the level of phospholylated-p70S6K by a Western blotting analysis (Fig. 5c). The phosphorylation of the threonine-389 residue of p70S6K by 50 μmol/L of GGA was detected. Similar to mTOR, the band intensity of phospho-threonine-389 of p70S6K decreased after pretreatment with rapamycin, but the intensity was almost the same as that seen following treatment with GGA alone after pretreatment with LY294002 (Fig. 5c).

Discussion

GGA demonstrated the anti-HCV activity in this study. The anti-HCV effect depended on the GGA induced mTOR activity, not STAT-1 activity. An additive effect was observed with the combination of IFN and GGA.

GGA is a non-toxic heat shock protein (HSP) 70 inducer [13]. Various GGA activities outside of the stomach are also related to HSP induction [14–16]. GGA induced HSP-70 exerts an anti-ischemic stress activity in the heart and liver [16, 17], an anti-inflammatory activity in various cell types [18] and promotes liver regeneration [19]. GGA induces thioredoxin as well as HSP-70 in hepatocytes and other cells [20]. Thioredoxin anti-virus activity, is induced by AP-1 and NF-κB but not HSP-70 [21]. GGA has potent

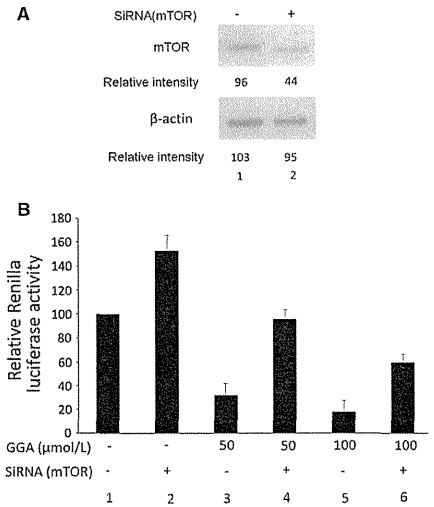

Fig. 4 Changes in GGA suppressed HCV replication by mTOR-siRNA. **a** OR6 cells were transfected with mTOR-siRNA (*lane 1*) or the non-targeted siRNA (*lane 2*). The expression of mTOR was evaluated by a Western blotting analysis. **b** The OR6 cells were transfected with mTOR-siRNA (*lanes 2, 4* and *6*) and the non-targeted siRNA (*lanes 1, 3* and *5*). One day later, the cells were treated with GGA (*lanes 3–6*). The HCV replicon assay is the same as Fig. 3. Non-treatment OR6 cells has 100% of relative *Renilla* luciferase light unit. The *Renilla* luciferase activity increased in the OR6 cells transfected with mTOR-siRNA (*lane 2*) in comparison to the non-targeted siRNA (*lane 1*). However, in OR6 cells treated with GGA, there was a greater elevation of *Renilla* luciferase activity in OR6 cells transfected with mTOR-siRNA (*lanes 4* and *6*) as compared to that with the non-targeted siRNA (*lanes 3* and *5*). The data are expressed as the mean ± SD and are representative example of four similar experiments

antiviral activity via the enhancement of antiviral factors and can clinically provide protection from influenza virus infection [22]. GGA significantly inhibits the synthesis of influenza virus-associated proteins and prominently enhances the expression of human myxovirus resistance 1 (MxA) followed by increased HSP-70 transcription [22]. Moreover, GGA augments the expression of an interferon-inducible double-strand RNA-activated protein kinase (PKR) gene and promotes PKR autophosphorylation and concomitantly alpha subunit of eukaryotic initiation factor 2 phosphorylation during influenza virus infection [22]. These anti-virus activities are related to GGA induced HSP-70. But, HSP-70 protein and PKR were not induced by GGA in OR6 cells in the current study. There is apparently no relationship between the GGA induced anti-HCV activity and HSP, PKR in OR6 cells. Therefore, we thought that HSP and PKR-independent anti-HCV activity induced by GGA was present in this hepatoma-derived cell line.

GGA induction of anti-viral protein is dependent upon STAT-1 tyrosine phosphorylation in HuH-7 and HepG2 [10]. However, GGA did not induce STAT-1 tyrosine phosphorylation and anti-virus protein, PKR, in OR6 cells in this study. Moreover, the GGA induced anti-HCV activity depended on mTOR activity, not STAT-1. OR6 cells are full length HCV replicon transfected HuH-7 cells [11]. HCV virus products inhibit the Jak-STAT pathway [23–25]. The mechanism of inhibition of the Jak-STAT pathway is multi-factorial including the suppressor of cytokine signaling 3 (SOCS-3) expression [26], protein phosphatase 2A (PP2A) induction [27], STAT-3 expression [28] and IL-8 expression [29]. GGA induced STAT-1 tyrosine phosphorylation and inducible PKR protein levels are also minor. Generally, the replicon transfection induces the intrinsic IFN [30], but STAT-1 tyrosine phosphorylation was not detected in combined OR6 cells. HCV replicon produced viral product might be inhibiting GGA-induced STAT-1 tyrosine phosphorylation.

mTOR is associated with the IFN induced anti-HCV signal [31]. The IFN activated mTOR pathway exhibits important regulatory effects in the generation of the IFN responses, including the anti-encephalomyocarditis virus effect [32]. IFN-induced mTOR is LY294002 sensitive and does not affect the IFN-stimulated regulatory element (ISRE) dependent promoter gene activity. A relationship has been observed between the replication of the hepatitis virus and mTOR activity. p21-activated kinase 1 is activated through the mTOR/p70 S6 kinase pathway and regulates the replication of HCV [33]. The IFN induced mTOR activity, independent of PI3K and Akt, is the critical factor for its anti-HCV activity and Jak independent TOR activity involves STAT-1 phosphorylation and nuclear localization, and then PKR is expressed in hepatocytes [31]. No relationship between GGA and mTOR has been reported. However, GGA induced anti-HCV activity depended on mTOR activity independent of PI3-K-Akt, as observed with IFN induced mTOR activity.

When 150 mg of GGA was administered orally, the serum concentration of GGA was approximately 7 μmol/L [34]. The concentration of GGA in the portal blood would be several-fold higher than the serum concentration of GGA; therefore, we speculated that the pharmacological action that would be obtained in clinical practice would be the same as that observed in this study.

GGA, a drug that can be safely administered orally, has mTOR dependent anti-HCV activity. The combination of IFN and GGA has an additive effect on anti-HCV activity. The current results suggest that combination therapy with GGA and IFN is, therefore, expected to improve the anti-HCV activity. It will, therefore, be necessary to examine the clinical effectiveness of the combination with GGA and IFN for HCV patients in the future.

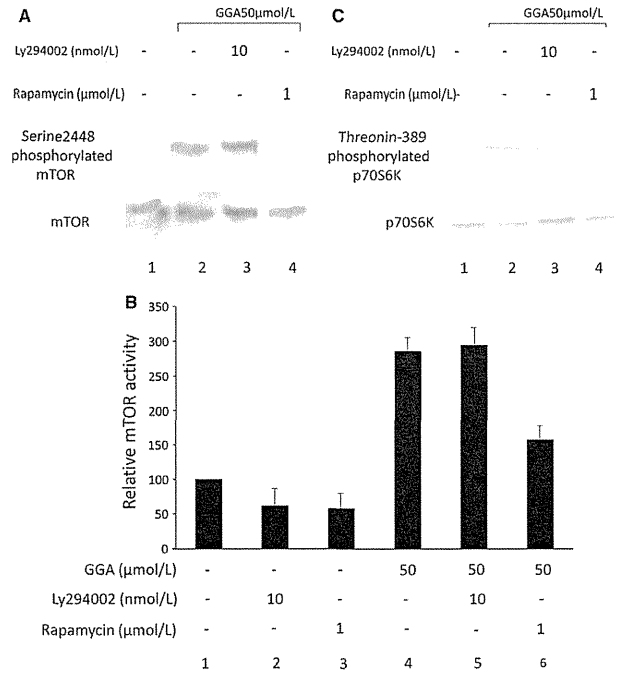

Fig. 5 Effect of GGA on mTOR and effect of LY294002 and rapamycin on GGA-induced serine phosphorylated mTOR and threonine phosphorylated p70S6K. **a** After pretreatment with 10 nmol/L LY294002 (*lane 3*) and 1 μmol/L rapamycin (*lane 4*) for 3 h, the OR6 cells were either untreated (*lane 1*) or treated with 50 μmol/L GGA (*lanes 2–4*) for 30 min and then were phosphorylated mTOR at serine-2448 residue (*upper panel*), the expression of mTOR (*lower panel*) was analyzed by Western blotting. **b** After pretreatment with 10 nmol/L LY294002 (*lanes 2* and *5*) and 1 μmol/L rapamycin (*lanes 3* and *6*) for 3 h, the OR6 cells were either untreated (*lanes 1–3*) or treated with 50 μmol/L GGA (*lanes 4–6*) for 30 min. The mTOR kinase activity was determined by ELISA-based mTOR kinase activity assay kit ($n = 4$). The differences between *lanes 1* and *4*, *lanes 4* and *6*, and *lanes 5* and *6* were statistically significant. The data are expressed as the mean ± SD and are representative of four similar experiments. **c** After pretreatment with 10 nmol/L LY294002 (*lane 3*) and 1 μmol/L, and with rapamycin (*lane 4*) for 3 h, the OR6 cells were either untreated (*lane 1*) or treated with 50 μmol/L GGA (*lanes 2–4*) for 30 min, and then were examined for phosphorylated p70S6K at the threonine-389 residue (*upper panel*), or the expression of p70S6K (*lower panel*) by a Western blotting analysis

References

1. Fattovich G, Stroffolini T, Zagni I, Donato F. Hepatocellular carcinoma in cirrhosis: incidence and risk factors. Gastroenterology. 2004;127:S35–50.
2. Pawlotsky JM, Chevaliez S, McHutchison JG. The hepatitis C virus life cycle as a target for new antiviral therapies. Gastroenterology. 2007;132:1979–98.
3. Murakami M, Oketani K, Fujisaki H, Wakabayashi T, Ohgo T. Antiulcer effect of geranylgeranylacetone, a new acyclic polyisoprenoid, on experimentally induced gastric and duodenal ulcers in rats. Arzneimittelforschung. 1981;31:799–804.
4. Murakami M, Oketani K, Fujisaki H, Wakabayashi T, Inai Y, Abe S, et al. Effect of synthetic acyclic polyisoprenoids on the cold-restraint stress induced gastric ulcer in rats. Jpn J Pharmacol. 1983;33:549–56.
5. Hirakawa T, Rokutan K, Nikawa T, Kishi K. Geranylgeranylacetone induces heat shock proteins in cultured guinea pig gastric mucosal cells and rat gastric mucosa. Gastroenterology. 1996;111:345–57.
6. Sakai I, Tanaka T, Osawa S, Hashimoto S, Nakaya K. Geranylgeranylacetone used as an antiulcer agent is a potent inducer of differentiation of various human myeloid leukemia cell lines. Biochem Biophys Res Commun. 1993;191:873–9.

7. Okada S, Yabuki M, Kanno T, Hamazaki K, Yoshioka T, Yasuda T, et al. Geranylgeranylacetone induces apoptosis in HL-60 cells. Cell Struct Funct. 1999;24:161–8.
8. Araki H, Shidoji Y, Yamada Y, Moriwaki H, Muto Y. Retinoid agonist activities of synthetic geranyl geranoic acid derivatives. Biochem Biophys Res Commun. 1995;209:66–72.
9. Kuhen KL, Vessey JW, Samuel CE. Mechanism of interferon action: identification of essential positions within the novel 15-base-pair KCS element required for transcriptional activation of the RNA-dependent protein kinase PKR gene. J Virol. 1998; 72:9934–9.
10. Ichikawa T, Nakao K, Nakata K, Hamasaki K, Takeda Y, Kajiya Y, et al. Geranylgeranylacetone induces antiviral gene expression in human hepatoma cells. Biochem Biophys Res Commun. 2001; 280:933–9.
11. Ikeda M, Abe K, Dansako H, Nakamura T, Naka K, Kato N. Efficient replication of a full-length hepatitis C virus genome, strain O, in cell culture, and development of a luciferase reporter system. Biochem Biophys Res Commun. 2005;329:1350–9.
12. Tanaka H, Samuel CE. Mechanism of interferon action. Structure of the mouse PKR gene encoding the interferon-inducible RNA-dependent protein kinase. Proc Natl Acad Sci USA. 1994;91: 7995–9.
13. Hirakawa T, Rokutan K, Nikawa T, Kishi K. Geranylgeranylacetone induces heat shock proteins in cultured guinea pig gastric mucosal cells and rat gastric mucosa. Gastroenterology. 1996; 111:345–57.
14. Uchida S, Fujiki M, Nagai Y, Abe T, Kobayashi H. Geranylgeranylacetone, a noninvasive heat shock protein inducer, induces protein kinase C and leads to neuroprotection against cerebral infarction in rats. Neurosci Lett. 2006;396:220–4.
15. Fujibayashi T, Hashimoto N, Jijiwa M, Hasegawa Y, Kojima T, Ishiguro N. Protective effect of geranylgeranylacetone, an inducer of heat shock protein 70, against drug-induced lung injury/fibrosis in an animal model. BMC Pulm Med. 2009;9:45.
16. Sakabe M, Shiroshita-Takeshita A, Maguy A, Brundel BJ, Fujiki A, Inoue H, et al. Effects of a heat shock protein inducer on the atrial fibrillation substrate caused by acute atrial ischaemia. Cardiovasc Res. 2008;78:63–70.
17. Fudaba Y, Ohdan H, Tashiro H, Ito H, Fukuda Y, Dohi K, et al. Geranylgeranylacetone, a heat shock protein inducer, prevents primary graft nonfunction in rat liver transplantation. Transplantation. 2001;72:184–9.
18. Mochida S, Matsura T, Yamashita A, Horie S, Ohata S, Kusumoto C, et al. Geranylgeranylacetone ameliorates inflammatory response to lipopolysaccharide (LPS) in murine macrophages: inhibition of LPS binding to the cell surface. J Clin Biochem Nutr. 2007;41:115–23.
19. Kanemura H, Kusumoto K, Miyake H, Tashiro S, Rokutan K, Shimada M. Geranylgeranylacetone prevents acute liver damage after massive hepatectomy in rats through suppression of a CXC chemokine GRO1 and induction of heat shock proteins. J Gastrointest Surg. 2009;13:66–73.
20. Hirota K, Nakamura H, Arai T, Ishii H, Bai J, Itoh T, et al. Geranylgeranylacetone enhances expression of thioredoxin and suppresses ethanol-induced cytotoxicity in cultured hepatocytes. Biochem Biophys Res Commun. 2000;275:825–30.
21. Schenk H, Klein M, Erdbrügger W, Dröge W, Schulze-Osthoff K. Distinct effects of thioredoxin and antioxidants on the activation of transcription factors NF-kappa B and AP-1. Proc Natl Acad Sci USA. 1994;91:1672–6.
22. Unoshima M, Iwasaka H, Eto J, Takita-Sonoda Y, Noguchi T, Nishizono A. Antiviral effects of geranylgeranylacetone: enhancement of MxA expression and phosphorylation of PKR during influenza virus infection. Antimicrob Agents Chemother. 2003;47:2914–21.
23. Lin W, Choe WH, Hiasa Y, Kamegaya Y, Blackard JT, Schmidt EV, et al. Hepatitis C virus expression suppresses interferon signaling by degrading STAT1. Gastroenterology. 2005;128:1034–41.
24. Lan KH, Lan KL, Lee WP, Sheu ML, Chen MY, Lee YL, et al. HCV NS5A inhibits interferon-alpha signaling through suppression of STAT1 phosphorylation in hepatocyte-derived cell lines. J Hepatol. 2007;46:759–67.
25. Luquin E, Larrea E, Civeira MP, Prieto J, Aldabe R. HCV structural proteins interfere with interferon-alpha Jak/STAT signalling pathway. Antiviral Res. 2007;76:194–7.
26. Huang Y, Feld JJ, Sapp RK, Nanda S, Lin JH, Blatt LM, et al. Defective hepatic response to interferon and activation of suppressor of cytokine signaling 3 in chronic hepatitis C. Gastroenterology. 2007;132:733–44.
27. Duong FH, Filipowicz M, Tripodi M, La Monica N, Heim MH. Hepatitis C virus inhibits interferon signaling through up-regulation of protein phosphatase 2A. Gastroenterology. 2004;126: 263–77.
28. Brender C, Lovato P, Sommer VH, Woetmann A, Mathiesen AM, Geisler C, et al. Constitutive SOCS-3 expression protects T-cell lymphoma against growth inhibition by IFNalpha. Leukemia. 2005;19:209–13.
29. Jia Y, Wei L, Jiang D, Wang J, Cong X, Fei R. Antiviral action of interferon-alpha against hepatitis C virus replicon and its modulation by interferon-gamma and interleukin-8. J Gastroenterol Hepatol. 2007;22:1278–85.
30. Fredericksen B, Akkaraju GR, Foy E, Wang C, Pflugheber J, Chen ZJ, et al. Activation of the interferon-beta promoter during hepatitis C virus RNA replication. Viral Immunol. 2002;15: 29–40.
31. Matsumoto A, Ichikawa T, Nakao K, Miyaaki H, Hirano K, Fujimito M, et al. Interferon-alpha-induced mTOR activation is an anti-hepatitis C virus signal via the phosphatidylinositol 3-kinase-Akt-independent pathway. J Gastroenterol. 2009;44: 856–63.
32. Kaur S, Lal L, Sassano A, Majchrzak-Kita B, Srikanth M, Baker DP, et al. Regulatory effects of mammalian target of rapamycin activated pathways in type I and II interferon signaling. J Biol Chem. 2007;282:1757–68.
33. Ishida H, Li K, Yi M, Lemon SM. p21-activated kinase 1 is activated through the mammalian target of rapamycin/p70 S6 kinase pathway and regulates the replication of hepatitis C virus in human hepatoma cells. J Biol Chem. 2007;282:11836–48.
34. Hasegawa J, Morishita N, Seki T, Hashida N, Kanazawa T, Sato A. Effect of meals in healthy adult administered Selbex. Syokakika. 1987;7:740–52.

Virus Genes
DOI 10.1007/s11262-012-0712-2

Development of a drug assay system with hepatitis C virus genome derived from a patient with acute hepatitis C

Kyoko Mori · Youki Ueda · Yasuo Ariumi · Hiromichi Dansako · Masanori Ikeda · Nobuyuki Kato

Received: 5 October 2011 / Accepted: 1 January 2012

Abstract We developed a new cell culture drug assay system (AH1R), in which genome-length hepatitis C virus (HCV) RNA (AH1 strain of genotype 1b derived from a patient with acute hepatitis C) efficiently replicates. By comparing the AH1R system with the OR6 assay system that we developed previously (O strain of genotype 1b derived from an HCV-positive blood donor), we demonstrated that the anti-HCV profiles of reagents including interferon-γ and cyclosporine A significantly differed between these assay systems. Furthermore, we found unexpectedly that rolipram, an anti-inflammatory drug, showed anti-HCV activity in the AH1R assay but not in the OR6 assay, suggesting that the anti-HCV activity of rolipram differs depending on the HCV strain. Taken together, these results suggest that the AH1R assay system is useful for the objective evaluation of anti-HCV reagents and for the discovery of different classes of anti-HCV reagents.

Keywords HCV · Acute hepatitis C · Anti-HCV drug assay system · Anti-HCV activity of rolipram

Introduction

Hepatitis C virus (HCV) infection frequently causes chronic hepatitis, which progresses to liver cirrhosis and hepatocellular carcinoma. HCV is an enveloped virus with a positive single-stranded 9.6 kb RNA genome, which encodes a large polyprotein precursor of approximately 3,000 amino acid (aa) residues [1, 2]. This polyprotein is cleaved by a combination of the host and viral proteases into at least 10 proteins in the following order: Core, envelope 1 (E1), E2, p7, non-structural 2 (NS2), NS3, NS4A, NS4B, NS5A, and NS5B [1].

Human hepatoma HuH-7 cell culture-based HCV replicon systems derived from a number of HCV strains have been widely used for various studies on HCV RNA replication [3, 4] since the first replicon system (based on the Con1 strain of genotype 1b) was developed in 1999 [5]. Genome-length HCV RNA replication systems (see Fig. 2 for details) derived from a limited number of HCV strains (H77, N, Con1, O, and JFH-1) are also sometimes used for such studies, as they are more useful than the replicon systems lacking the structural region of HCV, although the production of infectious HCV from the genome-length HCV RNA has not been demonstrated to date [3, 4]. Furthermore, these RNA replication systems have been improved enough to be suitable for the screening of anti-HCV reagents by the introduction of reporter genes such as luciferase [3, 4, 6]. We also developed an HuH-7-derived cell culture assay system (OR6) in which genome-length HCV RNA (O strain of genotype 1b derived from an HCV-positive blood donor) encoding renilla luciferase (RL) efficiently replicates [7]. Such reporter assay systems could save time and facilitate the mass screening of anti-HCV reagents, since the values of luciferase correlated well with the level of HCV RNA after treatment with anti-HCV reagents. Furthermore, OR6 assay system became more useful as a drug assay system than the HCV subgenomic replicon-based reporter assay systems developed to date [3, 4], because the older systems lack the Core-NS2 regions containing structural proteins likely to be involved in the events that take place in the HCV-infected human liver.

K. Mori · Y. Ueda · Y. Ariumi · H. Dansako · M. Ikeda · N. Kato (✉)
Department of Tumor Virology, Okayama University Graduate School of Medicine, Dentistry, and Pharmaceutical Sciences, 2-5-1 Shikata-cho, Okayama 700-8558, Japan
e-mail: nkato@md.okayama-u.ac.jp

Published online: 18 January 2012

Indeed, by the screening of preexisting drugs using the OR6 assay system, we have identified mizoribine [8], statins [9], hydroxyurea [10], and teprenone [11] as new anti-HCV drug candidates, indicating that the OR6 assay system is useful for the discovery of anti-HCV reagents.

On the other hand, we previously established for the first time an HuH-7-derived cell line (AH1) that harbors genome-length HCV RNA (AH1 strain of genotype 1b) derived from a patient with acute hepatitis C [12]. In that study, we noticed different anti-HCV profiles of interferon (IFN)-γ or cyclosporine A (CsA) between AH1 and O cells supporting genome-length HCV RNA (O strain) replication [7]. From these results, we supposed that the diverse effects of IFN-γ or CsA were attributable to the difference in HCV strains [12].

To test this assumption in detail, we first developed an AH1 strain-derived assay system (AH1R) corresponding to the OR6 assay system, and then performed a comparative analysis using AH1R and OR6 assay systems. In this article, we report that the difference in HCV strains causes the diverse effects of anti-HCV reagents, and we found unexpectedly by AH1R assay that rolipram, an anti-inflammatory drug, is an anti-HCV drug candidate.

Materials and methods

Reagents

IFN-α, IFN-γ, and CsA were purchased from Sigma-Aldrich (St. Louis, MO). Rolipram was purchased from Wako Pure Chemical Industries (Osaka, Japan).

Plasmid construction

The plasmid pAH1RN/C-5B/PL,LS,TA,$(VA)_3$ was constructed from pAH1 N/C-5B/PL,LS,TA,$(VA)_3$ encoding genome-length HCV RNA clone 2 (See Fig. 2) obtained from AH1 cells [12], by introducing a fragment of the RL gene from pORN/C-5B into the *Asc*I site before the neomycin phosphotransferase (Neo^R) gene as previously described [7].

RNA synthesis

The plasmid pAH1RN/C-5B/PL,LS,TA,$(VA)_3$ DNA was linearized by *Xba*I, and used for RNA synthesis with T7 MEGAscript (Ambion, Austin TX) as previously described [7].

Cell cultures

AH1R and OR6 cells supporting genome-length HCV RNAs were cultured in Dulbecco's modified Eagle's medium (DMEM) supplemented with 10% fetal bovine serum (FBS) and 0.3 mg/mL of G418 (Geneticin; Invitrogen, Carlsbad, CA). AH1c-cured cells, which were created by eliminating HCV RNA from AH1 cells [12] by IFN-γ treatment, were also cultured in DMEM supplemented with 10% FBS.

RNA transfection and selection of G418-resistant cells

Genome-length HCV (AH1RN/C-5B/PL,LS,TA,$(VA)_3$) RNA synthesized in vitro was transfected into AH1c cells by electroporation, and the cells were selected in the presence of G418 (0.3 mg/mL) for 3 weeks as described previously [13].

RL assay for anti-HCV reagents

To monitor the effects of anti-HCV reagents, RL assay was performed as described previously [14]. Briefly, the cells were plated onto 24-well plates (2×10^4 cells per well) in triplicate and cultured with the medium in the absence of G418 for 24 h. The cells were then treated with each reagent at several concentrations for 72 h. After treatment, the cells were subjected to a luciferase assay using the RL assay system (Promega, Madison, WI). From the assay results, the 50% effective concentration (EC_{50}) of each reagent was determined.

Quantification of HCV RNA

Quantitative reverse transcription-polymerase chain reaction (RT-PCR) analysis for HCV RNA was performed using a real-time LightCycler PCR (Roche Applied Science, Indianapolis, IN, USA) as described previously [7]. The experiments were done in triplicate.

IFN-α treatment to evaluate the assay systems

To monitor the anti-HCV effect of IFN-α on AH1R cells, 2×10^4 cells and 5×10^5 cells were plated onto 24-well plates (for luciferase assay) and 10 cm plates (for quantitative RT-PCR assay) in triplicate, respectively, and cultured for 24 h. The cells were then treated with IFN-α at final concentrations of 0, 1, 10, and 100 IU/mL for 24 h, and subjected to luciferase and quantitative RT-PCR assays as described above.

Western blot analysis

The preparation of cell lysates, sodium dodecyl sulfate–polyacrylamide gel electrophoresis, and immunoblotting analysis with a PVDF membrane were performed as described previously [13]. The antibodies used in this study were those against HCV Core (CP11 monoclonal antibody; Institute of Immunology, Tokyo), NS5B, and E2 (generous gifts from Dr. M. Kohara, Tokyo Metropolitan Institute of Medical Science, Japan). Anti-β-actin antibody (AC-15; Sigma, St. Louis, MO, USA) was used as a control for the amount of protein loaded per lane. Immunocomplexes were detected with the Renaissance enhanced chemiluminescence assay (Perkin-Elmer Life Sciences, Boston, MA).

WST-1 cell proliferation assay

The cells were plated onto 96-well plates (1×10^3 cells per well) in triplicate and then treated with rolipram at several concentrations for 72 h. After treatment, the cells were subjected to the WST-1 cell proliferation assay (Takara Bio, Otsu, Japan) according to the manufacturer's protocol. From the assay results, the 50% cytotoxic concentration (CC_{50}) of rolipram was estimated. The selective index (SI) value of rolipram was also estimated by dividing the CC_{50} value by the EC_{50} value.

RT-PCR and sequencing

To amplify the genome-length HCV RNA, RT-PCR was performed separately in two fragments as described previously [7, 15]. Briefly, one fragment covered from 5′-untranslated region to NS3, with a final product of approximately 6.2 kb, and the other fragment covered from NS2 to NS5B, with a final product of approximately 6.1 kb. These fragments overlapped at the NS2 and NS3 regions and were used for sequence analysis of the HCV open reading frame (ORF) after cloning into pBR322MC. PrimScript (Takara Bio) and KOD-plus DNA polymerase (Toyobo, Osaka, Japan) were used for RT and PCR, respectively. The nucleotide sequences of each of the three independent clones obtained were determined using the Big Dye terminator cycle sequencing kit on an ABI PRISM 310 genetic analyzer (Applied Biosystems, Foster City, CA, USA).

Statistical analysis

Differences between AH1R and OR6 cell lines were tested using Student's t test. P values <0.05 were considered statistically significant.

Results

Development of a luciferase reporter assay system that facilitates the quantitative monitoring of genome-length HCV-AH1 RNA replication

To develop an HCV AH1 strain-derived assay system corresponding to the OR6 assay system [7], a genome-length HCV RNA encoding RL (AH1RN/C-5B/PL,LS,TA,$(VA)_3$) was transfected into AH1c cells. Following 3 weeks of culturing in the presence of G418, more than 10 colonies were obtained, and then 8 colonies (#2, #3, #4, #5, #6, #8, #13, and #14) were successfully proliferated. We initially selected colonies #2, #3, and #14 because they had high levels of RL activity ($>4 \times 10^6$ U/1.6×10^5 cells) (Fig. 1a). However, RT-PCR and the sequencing analyses revealed that the genome-length HCV-AH1 RNAs obtained from these colonies each had an approximately 1 kb deletion in the E2 region (data not shown). In this regard, we previously observed similar phenomenon and described the difficulty of the development of a luciferase reporter assay system using the genome-length HCV RNA of more than 12 kb [7], suggesting that the NS5B polymerase possesses the limited elongation ability (probably up to a total length of 12 kb). Indeed, in that study, we could overcome this obstacle by the selection of the colony harboring a complete genome-length HCV RNA among the obtained G418-resistant colonies [7]. Therefore, we next carried out the selection among the other colonies. Fortunately, we found that colony #4, showing a rather high level of RL activity (2×10^6 U/1.6×10^5 cells), possessed a complete genome-length HCV-AH1 RNA without any deleted forms, although most of the other colonies possessed some amounts of a deleted form in addition to a complete genome-length HCV-AH1 RNA (data not shown). We demonstrated that the HCV RNA sequence was not integrated into the genomic DNA in colony #4 (data not shown). From these results, we finally selected colony #4, and it was thereafter referred to as AH1R and used for the following studies.

We first demonstrated that AH1R cells expressed sufficient levels of HCV proteins (Core, E2, and NS5B) by Western blot analysis for the evaluation of anti-HCV reagents, and the expression levels were almost equivalent to those in OR6 cells (Fig. 1b). In this analysis, we confirmed that the size of the E2 protein in AH1R cells was 7 kDa larger than that in OR6 cells (Fig. 1b), as observed previously [12]. This result indicates that AH1R cells express AH1 strain-derived E2 protein possessing two extra N-glycosylation sites [12]. We next demonstrated good correlations between the levels of RL activity and HCV RNA in AH1R cells (Fig. 1c), as we previously demonstrated in OR6 cells treated with IFN-α for 24 h [7]. These correlations indicate that AH1R cells were as useful as OR6 cells as a luciferase assay system.

Aa substitutions detected in genome-length HCV RNA in AH1R cells

To examine whether or not genome-length HCV RNA in AH1R cells possesses additional conserved mutations such as adaptive mutations, we performed a sequence analysis of HCV RNA in AH1R cells. The results (Fig. 2) revealed that

Virus Genes

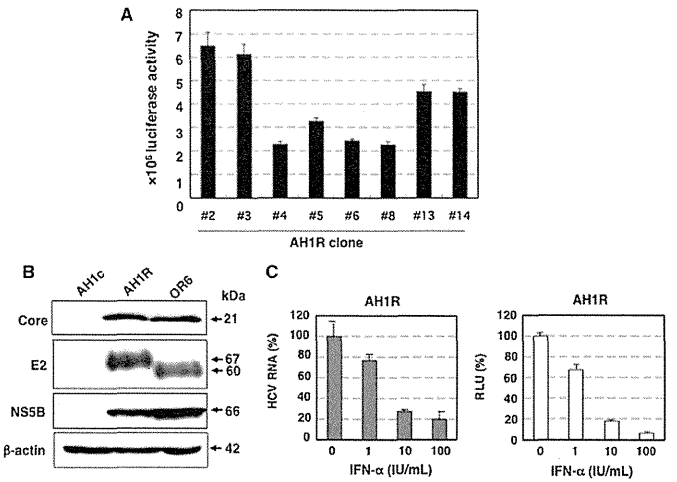

Fig. 1 Characterization of AH1R cells harboring genome-length HCV RNA. **a** Selection of G418-resistant cell clones. The levels of HCV RNA in G418-resistant cells were monitored by RL assay. **b** Western blot analysis. AH1c, AH1R, and OR6 cells were used for the comparison. *Core*, *E2*, and *NS5B* were detected by Western blot analysis. β-actin was used as a control for the amount of protein loaded per lane. **c** RL activity is correlated with HCV RNA level. The AH1R cells were treated with IFN-α (0, 1, 10, and 100 IU/mL) for 24 h, and then a luciferase reporter assay (*right panel*) and quantitative RT-PCR (*left panel*) were performed. The relative luciferase activity (RLU) (%) or HCV RNA (%) calculated at each point, when the level of luciferase activity or HCV RNA in non-treated cells was assigned to be 100%, is presented here

two additional mutations accompanying aa substitutions (W860R (NS2) and A1218E (NS3)) were detected commonly among the three independent clones sequenced, suggesting that these additional mutations are required for the efficient replication or stability of genome-length HCV RNA. The P1115L (NS3), L1262S (NS3), V1897A (NS4B), and V2360A (NS5A) mutations derived from the sAH1 replicon [12] were conserved in AH1R cell-derived clones. However, AH1-clone-2-specific mutations (T1338A and V1880A) were almost reverted to the consensus sequences of AH1 RNA [12] except for V1880A in AH1R clone 2 (Fig. 2). In addition, the Q63R (Core) mutation was observed in two of three clones (Fig. 2).

Comparison between the AH1R and OR6 assay systems regarding the sensitivities to IFN-α, IFN-γ, and CsA

Using quantitative RT-PCR analysis, we previously examined the anti-HCV activities of IFN-α, IFN-γ, and CsA in AH1 and O cells, and noticed different anti-HCV profiles of IFN-γ and CsA between AH1 and O cells [12]. In that study, AH1 cells seemed to be more sensitive than the O cells to CsA (significant difference was observed when 0.063, 0.12, or 0.25 μg/mL of CsA was used). Conversely, AH1 cells seemed to be less sensitive than the O cells to IFN-γ (significant difference was observed when 1 or 10 IU/mL of IFN-γ was used). However, we were not able to determine precisely the EC_{50} values of these reagents, because of the unevenness of the data obtained by RT-PCR.

After developing the AH1R assay system in this study, we determined the EC_{50} values of IFN-α, IFN-γ, and CsA using the AH1R assay and compared the values with those obtained by the OR6 assay. The results revealed that AH1R assay was more sensitive than OR6 assay to IFN-α (EC_{50}; 0.31 IU/mL for AH1R, 0.45 IU/mL for OR6) (Fig. 3a) and CsA (EC_{50}; 0.11 μg/mL for AH1R, 0.42 μg/mL for OR6) (Fig. 3b), and that the OR6 assay was more sensitive than the AH1R assay to IFN-γ (EC_{50}; 0.69 IU/mL for AH1R, 0.28 IU/mL for OR6) (Fig. 3c). Regarding these anti-HCV reagents, the anti-HCV activities observed between the AH1R and OR6 assays differed significantly in all of the concentrations examined (Fig. 3). In addition, regarding these anti-HCV reagents, cell growth was not suppressed within the concentrations used. Regarding IFN-γ and CsA, the present results clearly support those of our previous

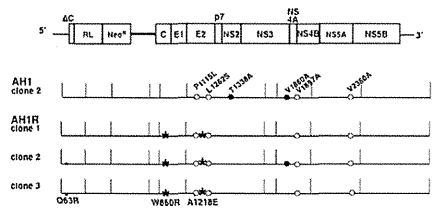

Fig. 2 Aa substitutions detected in intracellular AH1R genome-length HCV RNA. The *upper portion* shows schematic gene organization of genome-length HCV RNA encoding the *RL* gene developed in this study. Genome-length HCV RNA consists of 2 cistrons. In the first cistron, RL is translated as a fusion protein with Neo^R by HCV-IRES, and in the second cistron, all of HCV proteins (C-NS5B) are translated by encephalomyocarditis virus (EMCV)-IRES introduced in the region upstream of C-NS5B regions. Genome-length HCV RNA-replicating cells possess the G418-resistant phenotype because Neo^R is produced by the efficient replication of genome-length HCV RNA. Therefore, when genome-length HCV RNA is excluded from the cells or when its level is decreased, the cells are killed in the presence of G418. In this system, anti-HCV activity is able to evaluate the value of the reporter (RL activity) instead of the quantification of HCV RNA or HCV proteins. In addition, it has been known that the infectious HCV is not produced from this RNA replication system [3, 4, 6]. Core to NS5B regions of three independent clones (*AH1R clones 1–3*) sequenced are presented. W860R and A1218E conserved substitutions are indicated by *asterisks*. Q63R substitutions detected in two of three clones are each indicated by a *small dot*. Core to NS5B regions of *AH1 clone 2*, used to establish the AH1R cell line, are also presented. AH1-specific conserved substitutions and *AH1-clone-2*-specific substitutions are indicated by *open circles* and *black circles*, respectively

study [12]. Therefore, we suggest that the diverse effects of these anti-HCV reagents are due to the difference in HCV strains, although we are not able to completely exclude the possibility that AH1R cells are compromised cells causing the different responses against anti-HCV reagents. In summary, the previous and present findings suggest that the AH1R assay system is also useful for the evaluation of anti-HCV reagents as an independent assay system.

Anti-HCV activity of rolipram was clearly observed in the AH1R assay, but not in the OR6 assay

From the above findings, we supposed that the anti-HCV reagents reported to date might show diverse effects between the drug assay systems derived from the different HCV strains. To test this assumption, we used the AH1R and OR6 assay systems to evaluate the anti-HCV activity of more than 10 pre-existing drugs (6-Azauridine, bisindoly maleimide 1, carvedilol, cehalotaxine, clemizole, 2′-deoxy-5-fluorouridine, esomeprazole, guanazole, hemin, homoharringtonine, methotrexate, nitazoxanide, resveratrol, rolipram, silibinin A, Y27632, etc.), which other groups had evaluated using an assay system derived from the Con1 strain (genotype 1b) or JFH-1 strain (genotype 2a). The results revealed that most of these reagents in the AH1R assay showed similar levels of anti-HCV activities compared with those in the OR6 assay or those of the previous studies (data not shown). However, we found that only rolipram, a selective phosphodiesterase 4 (PDE4) inhibitor [16] that is used as an anti-inflammatory drug, showed moderate anti-HCV activity (EC_{50} 31 μM; CC_{50} > 200 μM; SI > 6) in the AH1R assay, but no such activity in the OR6 assay (upper panel in Fig. 4a). This remarkable difference was confirmed by Western blot analysis (lower panel in Fig. 4a). It is unlikely that rolipram's anti-HCV activity is due to the inhibition of exogenous RL, Neo^R or encephalomyocarditis virus internal ribosomal entry site (EMCV-IRES), all of which are encoded in the genome-length HCV RNA, because the AH1R and OR6 assay systems possess the same structure of genome-length HCV RNA except for HCV ORF. To demonstrate that rolipram's anti-HCV activity is not due to the clonal specificity of the cells or the specificity of genome-length HCV RNA, we examined the anti-HCV activity of rolipram using the monoclonal HCV replicon RNA-replicating cells (sAH1 cells for AH1 strain [12], and sO cells for O strain [13]). The results

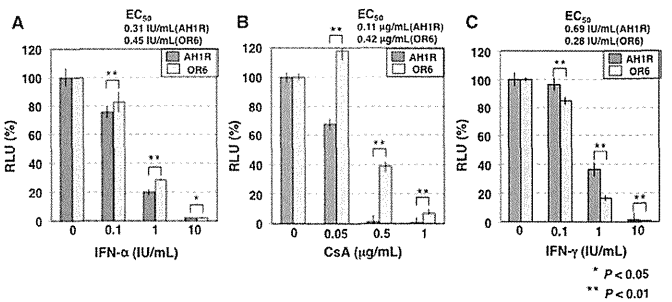

Fig. 3 The diverse effects of anti-HCV reagents on AH1R and OR6 assay systems. AH1R and OR6 cells were treated with anti-HCV reagents for 72 h, and then the RL assay was performed as described in Fig. 1c. **a** Effect of IFN-α. **b** Effect of CsA. **c** Effect of IFN-γ

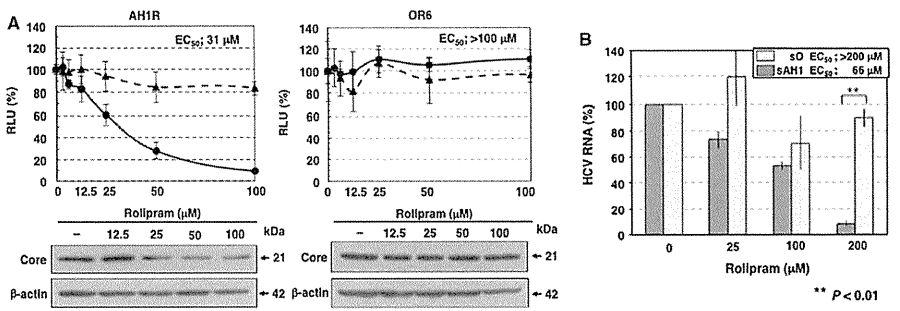

Fig. 4 Anti-HCV activity of rolipram. **a** Rolipram sensitivities on genome-length HCV RNA replication in AH1R and OR6 assay systems. AH1R and OR6 cells were treated with rolipram for 72 h, followed by RL assay (*black circle* with *linear line* in the *upper panels*) and WST-1 assay (*black triangle* with *broken line* in the *upper panels*). The relative value (%) calculated at each point, when the level in non-treated cells was assigned to 100%, is presented here. Western blot analysis of the treated cells for the HCV Core was also performed (*lower panels*). **b** Rolipram sensitivities on HCV replicon RNA replication in sAH1 and sO cells. sAH1 and sO cells were treated with rolipram for 72 h, and extracted total RNAs were subjected to quantitative RT-PCR for HCV 5′ untranslated region as described previously [7]. The HCV RNA (%) calculated at each point, when the level of HCV RNA in non-treated cells was assigned to be 100%, is presented here

revealed by quantitative RT-PCR that rolipram showed moderate anti-HCV activity (EC_{50} 66 μM) in sAH1 cells, but no such activity in sO cells (Fig. 4b). Anti-HCV activity of rolipram in sAH1 cells was a little weaker than that in AH1R cells (Fig. 4b). The similar phenomenon that the anti-HCV activity in genome-length HCV RNA-based reporter assay is stronger than that in HCV subgenomic replicon-based reporter assay was observed regarding other anti-HCV reagents in our previous studies [14, 17, 18]. This result suggests that the anti-HCV activity of rolipram is not either a clone-specific or genome-length HCV RNA-specific phenomenon. In our previous studies also [14, 18], we demonstrated that anti-HCV activities of several reagents including ribavirin and statins were not due to the clonal specificity of the cells. On the other hand, it was recently reported that rolipram did not show anti-HCV activity in the JFH-1 strain-derived assay [19]. Taken together, the previous and present results suggest that rolipram's anti-HCV activity differs depending on the HCV strain. In summary, rolipram was identified as a new anti-HCV candidate using the AH1R assay system.

Discussion

In the present study, we developed for the first time a drug assay system (AH1R), derived from the HCV-AH1 strain (from a patient with acute hepatitis C), in which HCV-AH1 RNA is efficiently replicated. Using this system, we found that rolipram, an anti-inflammatory drug, had potential anti-HCV activity. This potential had not been detected by preexisting assay systems such as OR6, in which HCV-O RNA was derived from an HCV-positive blood donor. Since an HCV replicon harboring the sAH1 cell line, the parent of the AH1R cell line, was obtained from OR6-cured cells [12], the divergence in rolipram's effects between AH1R and OR6 cells is probably attributable to the difference in HCV strains rather than to the difference in cell clones. Indeed, rolipram's anti-HCV activity was not observed in another ORL8 assay system (O strain), which was recently developed using a new hepatoma Li23 cell line (data not shown) [15]. Therefore, we propose that multiple assay systems derived from different HCV strains are required for the discovery of anti-HCV reagents such as rolipram or for the objective evaluation of anti-HCV activity.

Comparative evaluation analysis of anti-HCV activities of IFN-α, IFN-γ, and CsA using AH1-strain-derived AH1R and O-strain-derived OR6 assay systems demonstrated that each of these anti-HCV reagents showed significantly diverse antiviral effects between the two systems. Regarding IFN-γ and CsA, the present results obtained using a luciferase reporter assay fully supported our previous findings [12] using quantitative RT-PCR analysis. However, in the present analysis, we noticed that IFN-α also showed significantly diverse effects (especially at less than 1 IU/mL) between the AH1R and OR6 assays.

The differences in IFN-α sensitivity may be attributable to the difference in aa sequences in the IFN sensitivity-determining region (ISDR; aa 2209-2248 in the HCV-1b genotype), in which aa substitutions correlate well with IFN sensitivity in patients with chronic hepatitis C [20], because the AH1 strain possesses three aa substitutions (T2217A, H2218R, and A2224 V) in ISDR, whereas the O strain possesses no aa substitutions. However, no report has demonstrated the correlation between IFN sensitivity and the substitution numbers in ISDR using the cell culture-based HCV RNA replication system.

Alternatively, Akuta et al. [21] reported that aa substitutions at position 70 and/or position 91 in the HCV Core region of patients infected with the HCV-1b genotype are pretreatment predictors of null virological response (NVR) to pegylated IFN/ribavirin combination therapy. In particular, substitutions of arginine (R) by glutamine (Q) at position 70, and/or leucine (L) by methionine (M) at position 91, were common in NVR. The patients with position-70 substitutions often showed little or no decrease in HCV RNA levels during the early phase of IFN-α treatment [21]. Regarding this point, it is interesting that position 70 in the AH1 strain is R (wild type) and that in the O strain is Q (mutant type), whereas position 91 is L (wild type) in both strains. Therefore, wild-type R in position 70 of the AH1 strain may contribute to the high sensitivity to IFN-α in the AH1R assay. Regarding positions 70 and 91 of the HCV Core, it is noteworthy that, among all of the HCV strains used thus far to develop HCV replicon systems, only the AH1 strain possesses double wild-type aa (data not shown). Therefore, the AH1R assay system may be useful for further study of sensitivity to IFN/ribavirin treatment.

The anti-HCV activity of rolipram, which is currently used as an anti-inflammatory drug, is interesting, although its anti-HCV mechanism is unclear. As a selective PDE4 inhibitor [16], rolipram may attenuate fibroblast activities that can lead to fibrosis and may be particularly effective in the presence of transforming growth factor (TGF)-β1-induced fibroblast stimulation [22]. On the other hand, HCV enhances hepatic fibrosis progression through the generation of reactive oxygen species and the induction of TGF-β1 [23]. Taken together, the previous and present results suggest that rolipram may inhibit both HCV RNA replication and HCV-enhanced hepatic fibrosis. However, it is unclear that rolipram shows anti-HCV activity against the majority of HCV strains, because rolipram has been effective for AH1 strain, but not for O strain. Although rolipram's anti-HCV activity would be HCV-strain-specific, it is not clear which HCV strain is the major type regarding the sensitivity to rolipram. Since developed assay systems using genome-length HCV RNA-replicating cells are limited to several HCV strains including O and AH1 strains to date, further analysis using the assay systems of other HCV strains will be needed to clarify this point.

In this study, we demonstrated that the AH1R assay system, which was for the first time developed using an HCV strain derived from a patient with acute hepatitis C, showed different sensitivities against anti-HCV reagents in comparison with assay systems in current use, such as OR6 assay. Therefore, AH1R assay system would be useful for various HCV studies including the evaluation of anti-HCV reagents and the identification of antiviral targets.

Acknowledgment This study was supported by grants-in-aid for research on hepatitis from the Ministry of Health, Labor, and Welfare of Japan. K. M. was supported by a Research Fellowship for Young Scientists from the Japan Society for the Promotion of Science.

References

1. N. Kato, Acta Med. Okayama **55**, 133–159 (2001)
2. N. Kato, M. Hijikata, Y. Ootsuyama, M. Nakagawa, S. Ohkoshi, T. Sugimura, K. Shimotohno, Proc. Natl. Acad. Sci. USA **87**, 9524–9528 (1990)
3. R. Bartenschlager, S. Sparacio, Virus Res. **127**, 195–207 (2007)
4. D. Moradpour, F. Penin, C.M. Rice, Nat. Rev. Microbiol. **5**, 453–463 (2007)
5. V. Lohmann, F. Korner, J. Koch, U. Herian, L. Theilmann, R. Bartenschlager, Science **285**, 110–113 (1999)
6. M. Ikeda, N. Kato, Adv. Drug Deliv. Rev. **59**, 1277–1289 (2007)
7. M. Ikeda, K. Abe, H. Dansako, T. Nakamura, K. Naka, N. Kato, Biochem. Biophys. Res. Commun. **329**, 1350–1359 (2005)
8. K. Naka, M. Ikeda, K. Abe, H. Dansako, N. Kato, Biochem. Biophys. Res. Commun. **330**, 871–879 (2005)
9. M. Ikeda, K. Abe, M. Yamada, H. Dansako, K. Naka, N. Kato, Hepatology **44**, 117–125 (2006)
10. A. Nozaki, M. Morimoto, M. Kondo, T. Oshima, K. Numata, S. Fujisawa, T. Kaneko, E. Miyajima, S. Morita, K. Mori, M. Ikeda, N. Kato, K. Tanaka, Arch. Virol. **155**, 601–605 (2010)
11. M. Ikeda, Y. Kawai, K. Mori, M. Yano, K. Abe, G. Nishimura, H. Dansako, Y. Ariumi, T. Wakita, K. Yamamoto, N. Kato, Liver Int. **31**, 871–880 (2011)
12. K. Mori, K. Abe, H. Dansako, Y. Ariumi, M. Ikeda, N. Kato, Biochem. Biophys. Res. Commun. **371**, 104–109 (2008)
13. N. Kato, K. Sugiyama, K. Namba, H. Dansako, T. Nakamura, M. Takami, K. Naka, A. Nozaki, K. Shimotohno, Biochem. Biophys. Res. Commun. **306**, 756–766 (2003)
14. K. Mori, M. Ikeda, Y. Ariumi, H. Dansako, T. Wakita, N. Kato, Virus Res. **157**, 61–70 (2011)
15. N. Kato, K. Mori, K. Abe, H. Dansako, M. Kuroki, Y. Ariumi, T. Wakita, M. Ikeda, Virus Res. **146**, 41–50 (2009)
16. S.J. MacKenzie, M.D. Houslay, Biochem. J. **347**, 571–578 (2000)
17. M. Yano, M. Ikeda, K. Abe, H. Dansako, S. Ohkoshi, Y. Aoyagi, N. Kato, Antimicrob. Agents Chemother. **51**, 2016–2027 (2007)
18. G. Nishimura, M. Ikeda, K. Mori, T. Nakazawa, Y. Ariumi, H. Dansako, N. Kato, Antiviral Res. **82**, 42–50 (2009)
19. P. Gastaminza, C. Whitten-Baue, F.V. Chisari, Proc. Natl. Acad. Sci. USA **107**, 291–296 (2010)
20. N. Enomoto, I. Sakuma, Y. Asahina, M. Kurosaki, T. Murakami, C. Yamamoto, Y. Ogura, N. Izumi, F. Marumo, C. Sato, N. Engl. J. Med. **334**, 77–81 (1996)

21. N. Akuta, F. Suzuki, Y. Kawamura, H. Yatsuji, H. Sezaki, Y. Suzuki, T. Hosaka, M. Kobayashi, M. Kobayashi, Y. Arase, K. Ikeda, H. Kumada, J. Med. Virol. **79**, 1686–1695 (2007)
22. S. Togo, X. Liu, X. Wang, Am. J. Physiol. Lung Cell. Mol. Physiol. **296**, L959–L969 (2009)
23. W. Lin, W.L. Tsai, R.X. Shao, G. Wu, L.F. Peng, L.L. Barlow, W.J. Chung, L. Zhang, H. Zhao, J.Y. Jang, R.T. Chung, Gastroenterology **138**, 2509–2518 (2010)

MAJOR ARTICLE

Monoclonal Antibody 2-152a Suppresses Hepatitis C Virus Infection Through Betaine/GABA Transporter-1

Masaaki Satoh,[1] Makoto Saito,[1] Takashi Takano,[1,2] Yuri Kasama,[1] Tomohiro Nishimura,[1,3] Yasumasa Nishito,[4] Yuichi Hirata,[2] Masaaki Arai,[2] Masayuki Sudoh,[5] Chieko Kai,[5] Michinori Kohara,[2] and Kyoko Tsukiyama-Kohara[1]

[1]Department of Experimental Phylaxiology, Faculty of Life Sciences, Kumamoto University, Honjo Kumamoto City; [2]Department of Microbiology and Cell Biology, Tokyo Metropolitan Institute of Medical Science, Kamikitazawa, Setagaya-ku; [3]KAKETSUKEN, Kyokushi, Kikuchi, Kumamoto; [4]Center for Microarray Analysis, Tokyo Metropolitan Institute of Medical Science; [5]Kamakura Research Laboratories, Chugai Pharmaceutical Co., Ltd., Kajiwara, Kamakura-City, Kanagawa; and [6]Laboratory of Animal Research Center, Institute of Medical Science, University of Tokyo, Shirokane-dai Minato-Ku, Japan

Background. We recently established a monoclonal antibody (2-152a MAb) that binds to 3β-hydroxysterol-Δ24-reductase (DHCR24) by immunizing mice with cells (RzM6-LC) persistently expressing hepatitis C virus (HCV). Here, we aimed to analyze the activity of 2-152a MAb against HCV replication and explore the molecular mechanism underlying the antiviral activity.

Methods. We characterized the effects of 2-152a MAb on HCV replication and performed a microarray analysis of antibody-treated HCV replicon cells. The molecules showing a significant change after the antibody treatment were screened to examine their relationship with HCV replication.

Results. The antibody had antiviral activity both in vitro and in vivo (chimeric mice). In the microarray analysis, 2-152a MAb significantly suppressed the expression of betaine/GABA transporter-1 (BGT-1) in 2 HCV replicon cell lines but not in HCV-cured cells. Silencing of BGT-1 expression by small interfering RNA (siRNA) revealed significant suppression of HCV replication and infection without cytotoxicity. Further, BGT-1 expression was significantly increased in the presence of HCV ($P < .05$).

Conclusions. Our results suggest that 2-152a MAb suppresses HCV replication and infection through BGT-1. These findings highlight important roles of BGT-1 in HCV replication and reveal a possible target for anti-HCV therapy.

Hepatitis C virus (HCV) causes chronic hepatitis and hepatocellular carcinoma (HCC) [1–3]. Chronic HCV infection is a major global public health concern because it affects at least 170 million people worldwide [2]. The most effective treatment against HCV currently comprises a combination therapy of PEGylated α-interferon (IFN-α) and ribavirin [4, 5]. However, considering that sustained virological responses develop in only approximately half of the patients infected with HCV genotype 1, the clinical efficacy of this therapy is limited [6, 7]. Efforts to develop therapies against HCV are further hindered by the high level of viral variation and capacity of the virus to cause chronic infection. Therefore, there is an urgent need to develop effective treatments against chronic HCV infection.

In a previous study, we established a cell line expressing HCV (RzM6-LC) to investigate the effects of persistent HCV expression on cell growth [8]. We also established a monoclonal antibody (2-152a MAb) against the RzM6-LC cell line to produce clones that recognize both cell surface and intracellular molecules. Using this method, we identified 3b-hydroxysterol-D24-reductase (DHCR24) as the recognition molecule of this antibody.

Received 30 November 2010; accepted 10 May 2011.
Correspondence: Kyoko Tsukiyama-Kohara, PhD, DVM, Department of Experimental Phylaxiology, Faculty of Life Sciences, Kumamoto University, 1-1-1 Honjo, Kumamoto-shi, Kumamoto 860-8556, Japan (kkohara@kumamoto-u.ac.jp).

The Journal of Infectious Diseases 2011;204:1172–80

0022-1899 (print)/1537-6613 (online)/2011/2048-0005$14.00
DOI: 10.1093/infdis/jir501

DHCR24 (also termed seladin-1) is an enzyme that catalyzes the conversion of desmosterol to cholesterol in the postsqualene cholesterol biosynthetic pathway [9, 10]. DHCR24 also acts as a hydrogen peroxide scavenger [11]. Therefore, DHCR24 may play a crucial role in maintaining cell physiology through cholesterol synthesis and oxidative stress. We previously demonstrated that HCV infection upregulates DHCR24 expression, and overexpression of DHCR24 inhibits apoptosis and inactivates the tumor suppressor gene p53 [12]. Moreover, silencing of DHCR24 suppressed HCV replication [13]. However, the precise mechanisms through which DHCR24 affects the HCV life cycle are unclear. In this study, we aimed to analyze the activity of 2-152a MAb against HCV replication and explore the molecular mechanism underlying the antiviral activity.

Materials And Methods

Cell Lines and Reagents

Human hepatoma cell line HuH-7 cell-based HCV replicon-harboring cell lines [14] R6FLR-N (genotype 1b) [15], FLR3-1 (genotype 1b) [16], and JFH-1 (genotype 2a) [17] were maintained in Dulbecco's modified Eagle's medium (DMEM) GlutaMAX (Invitrogen) containing 10% fetal calf serum (FCS; Sigma-Aldrich) in the presence of G418 (500 mg/mL for R6FLR-N and FLR3-1, 300 mg/mL for JFH-1; Invitrogen). Cured/HuH-7 histone H3 lysine 4 (K4) cells cured off HCV by interferon treatment [18] were maintained in DMEM GlutaMAX containing 10% FCS without G418. The JFH/K4 cell line persistently infected with the HCV JFH-1 strain and HuH-7 cell lines were maintained in DMEM containing 10% FCS [19]. The human hepatoblastoma HepG2 cell line was also maintained in DMEM containing 10% FCS.

Generation of 2-152a MAb

BALB/c strain of mice was immunized with 7–8 intraperitoneal injections of RzM6-LC cells (5×10^6) in RIBI adjuvant (trehalose dimycolate + monophosphoryl lipid A emulsion; RIBI ImmunoChem Research). After completion of the immunization regimen, their spleens were excised and splenocytes were fused with mouse myeloma plasminogen activator inhibitor (PAI) cells by using PEG1500 (Roche). Hybridoma cells were then selected with hypoxanthine, aminopterin, and thymidine (Invitrogen), and culture supernatants were collected for screening by whole-cell enzyme-linked immunosorbent assay (ELISA).

HCV Infection in Humanized Chimeric Mouse Liver and HCV mRNA Quantification by Real-time Detection Polymerase Chain Reaction

We purchased (from PhoenixBio Co.) chimeric mice that were established by transplanting human primary hepatocytes into severely combined immunodeficient (SCID) mice carrying a urokinase plasminogen activator (uPA) transgene controlled by an albumin promoter [20]. These mice were then infected with plasma isolated before 2003 from an HCV-positive patient (HCR6) [8, 21], in accordance with the Declaration of Helsinki. The protocols for the animal experiments were preapproved by the local ethics committee, and the animals were maintained in accordance with the National Institutes of Health Guide for the Care and Use of Laboratory Animals. HCV genotype 1b RNA levels were established at $0.96–1.84 \times 10^7$ copies/mL in mouse serum samples before the antibody treatment. The antibody (2-152a MAb) and normal immunoglobin G (IgG, 400 mg/20 g body weight) were intraperitoneally injected into the mice (n = 4) at 2-day intervals over a period of 14 days. IFN-α (30 mg/kg) was administered subcutaneously at 2-day intervals over a period of 2 weeks. Human serum albumin in the blood of chimeric mice was measured by using an Alb-II kit according to the manufacturer's instructions (Eiken Chemical). HCV RNA levels in serum and JFH/K4 cells were measured by real-time detection polymerase chain reaction (real-time detection [RTD]-PCR) as described previously [22]. HCV RNA in the cell cultures and supernatants was extracted by using Isogene and Isogene LS (Nippon Gene), respectively.

Replication Assay Using HCV Replicon Cells

We used 3 HCV subgenomic replicon cell lines: R6FLR-N, FLR3-1, and JFH-1. They were seeded at a density of 5×10^3 cells/well in 96-well tissue culture plates in DMEM GlutaMAX (Invitrogen) containing 5% fetal bovine serum (Thermo Scientific). Following incubation for 24 hours at 37°C (in 5% CO_2), the medium was removed and serial dilutions of antibody were added. Luciferase activity was determined by using a Bright-Glo luciferase assay kit (Promega) after 72 hours according to the manufacturer's instructions. The results were calculated as the average percentage relative to the reactivity in untreated cells, which was set at 100%. The viability of the replicon cells was measured by using a WST-8 cell counting kit (Dojindo) according to the manufacturer's instructions.

Immunostaining and Antibodies

Cells were cultured on glass coverslips (1.0 cm diameter) and fixed with 1% paraformaldehyde in phosphate-buffered saline (PBS) at room temperature for 10 minutes in 24-well plates. To permeabilize the cell membranes, the cells were treated with 1% Triton X-100 in PBS at room temperature for 10 minutes. After washing with 0.05% Tween-20 in PBS, the cells were incubated with 2-152a MAb, antiprotein disulfate isomerase (PDI) rabbit polyclonal antibody (Stressgen Bioreagents) or normal mouse IgG for 1 hour and washed with 0.05% Tween-20 in PBS. Alexa Fluor 488-labeled goat antimouse IgG was used as the secondary antibody.

Anti-NS5A antibody was provided by Dr Yoshiharu Matsuura (Osaka University). Anti-myc mouse monoclonal antibody

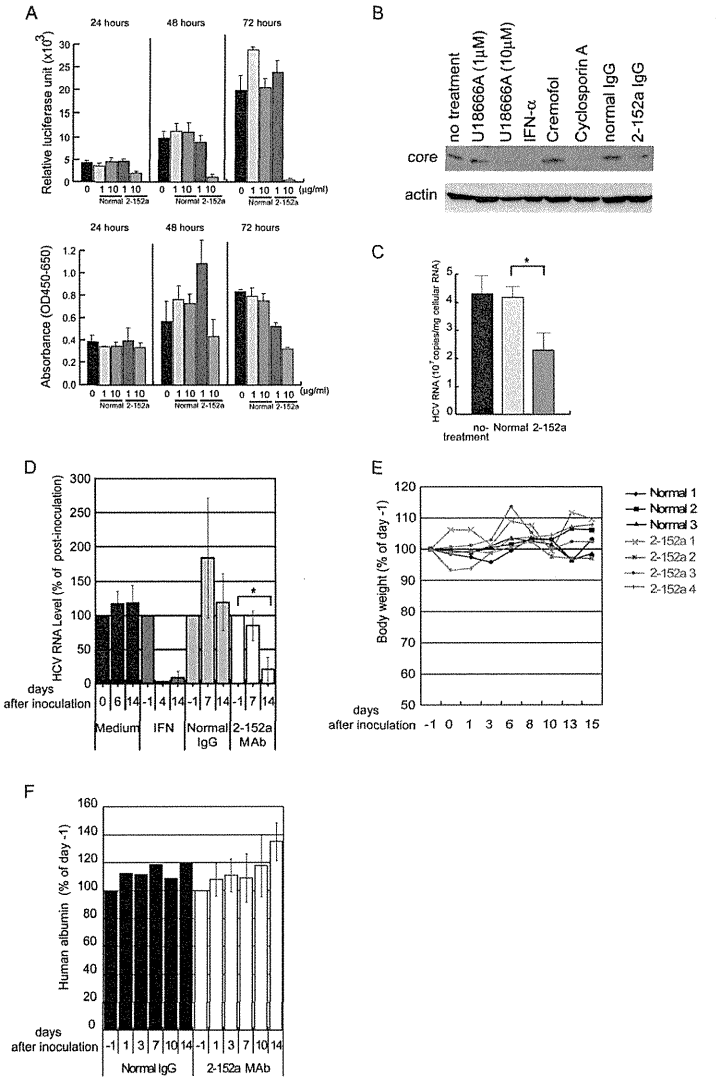

Figure 1. Anti-DHCR24 monoclonal antibody (2-152a MAb) suppresses HCV replication in vitro and in vivo. *A*, The effects of 2-152a MAb on HCV replication were measured by the luminescence activity and cell viability in FLR3-1 cells. The replicon cell line was incubated with IgG from normal mice or 2-152a MAb at 1 or 10 μg/mL for 24, 48, and 72 hours. The mean values from triplicate wells are indicated, and the vertical bars represent the standard deviation. The medium control (2% FCS-DMEM) without IgG is indicated as 0. *B*, The JFH/K4 cells were treated with cholesterol synthesis inhibitor U18666A (1 mM, 10 mM), IFN-α (250 IU/mL), Cyclosporin A (25 μM) and its solvent Cremophor, normal mouse IgG (10 μg/mL), and 2-152a IgG (10 μg/mL). HCV core and actin proteins were detected. *C*, HCV RNA copies were measured in JFH/K4 cells after treatment with normal or 2-152a IgG

(9E10; Cell Signaling Technology) and antiactin mouse monoclonal antibodies (Sigma-Aldrich) were utilized for detecting myc-fusion protein and normalization of the results, respectively.

cDNA Synthesis and Quantitative Reverse Transcriptase PCR

cDNA was synthesized from 0.5 or 1 mg of total RNA with a Superscript II kit (Invitrogen). TaqMan gene expression assays were custom designed and manufactured by Applied Biosystems. The expression was quantified with the ABI 7500 real-time PCR system (Applied Biosystems).

Microarray Analysis

For microarray analysis, total RNAs were extracted using RNAeasy kit (Qiagen), and RNA integrity was assessed using a Bioanalyzer (Agilent Technologies). cRNA targets were synthesized and hybridized with Whole Human Genome Oligo Microarray (G4112F; Agilent) according to the manufacturer's instructions.

RNA Interference, Expression Vector Construction, Transfection, and Rescue Experiments

Small interference RNA (siRNA) targeting betaine/GABA transporter-1 (BGT-1; nucleotides 120–144) was designed by using a program (https://rnaidesigner.invitrogen.com/) based on registered sequences in GenBank (5′-CAACAAGATGGAGT TTGTGCTGTCA-3′). Alternative siRNA (BGT-1-siRNA-362; nucleotides 362–386) was similarly designed. The HCV-siRNA (R7) sequence was 5′-GUCUCGUAGACCGUGCACCA dTdT-3′.

The coding region of the BGT-1 gene was obtained from RNA of R6FLR-N cells by reverse transcription–polymerase chain reaction (RT-PCR). The PCR products were inserted in *Eco*RV–*Xho*I sites of pcDNA6-myc His, version A (Invitrogen) after digestion of *Eco*RV–*Xho*I. To generate mutant plasmids that contained nucleotide substitutions in the siRNA-targeted site, we introduced point mutations into pcDNA-BGT-1 by using site-directed mutagenesis with a QuickChange multisite-directed mutagenesis kit (Stratagene), according to the manufacturer's instructions, and the following oligonucleotide primer: BGT-1-mut, 5′-CCAATGGACCAA-CAAGATGGAATTCGTTCTATCGGTGGCCGGGGAGCTC ATTGGG-3′ (the mutations introduced by mutagenesis are underlined).

Transfection of siRNAs was carried out by reverse transfection using Lipofectamine RNAiMAX according to the manufacturer's protocol (Invitrogen). Transfection of the expression vector was undertaken by using Lipofectamine LTX with Plus reagent (Invitrogen).

The rescue experiment was performed after reverse transfection of BGT-1 siRNA (1.5 nM) into R6FLR-N cells by using RNAiMAX reagent. After 48 hours, wild-type (wt) and mutant (mut) BGT-1 expression vectors (10 ng) were transfected by using Lipofectamine LTX, and the luciferase activity and cell viability were assessed by WST-8 assay (Dojindo) after 24 hours.

Analysis of HCV Infection and BGT-1 Expression

For infection assays, Cured/HuH-7 K4 cells were incubated with JFH/K4 cell-derived HCV (2.0×10^6 copies/mL). At 72 hours after incubation, HCV infection and BGT-1 expression were analyzed by real-time detection (RTD)-PCR and TaqMan expression assay, respectively, as described earlier.

Statistical Analysis

The Student *t* test was used to test the statistical significance of the results. *P* values $< .05$ were considered statistically significant.

Results

Inhibitory Effect of 2-152a MAb on HCV Replication In Vitro

We examined the effects of 2-152a MAb on HCV replication and the viability in HCV replicon cell lines. The treatment with 2-152a MAb significantly decreased HCV replication after 48 hours and cell viability after 72 hours (Figure 1*A*). To determine the recognition site of 2-152a MAb, we performed epitope mapping by using serial overlapping deletion mutants of the DHCR24 fusion protein (Supplementary Figure 1*A*). The recognition site was identified within amino acid residues 259–314 (Supplementary Figure 1*B*) and the predicted "Diminuto-like protein" homologous region [23] indicated in Supplementary Figure 1*A*.

Suppression of HCV Infection by 2-152a MAb

To determine the effects of 2-152a MAb on HCV infection, we inoculated the antibody into a persistently HCV-infected cell line (JFH/K4; Figure 1*B* and *C*) or uPA-SCID chimeric mice previously transplanted with human hepatocytes [20] and

Figure 1 continued. (10 μg/mL). The error bars indicate the standard deviation, and the asterisk indicates $P < .005$. *D*, Relative amounts of HCV RNA (% copies/mg total RNA on days −1 or 0) in the livers of chimeric mice inoculated with the control medium, PEGylated IFN-α, normal IgG, or 2-152a IgG were estimated by RTD-PCR. For normalization, the HCV RNA level 1 day before the inoculation (day −1) or on the day of inoculation (day 0) was defined as 100%. The graph shows the relative amounts of HCV RNA at −1 day (or day 0), 7 days (or 4 days), and 14 days. The error bars indicate the standard deviation, and the asterisk indicates $P < .005$. *E*, Ratio of body weight of mice inoculated with either normal IgG or 2-152a MAb IgG to that on day −1. *F*, Ratio of albumin concentration in serum samples of mice inoculated with 2-152a MAb IgG or normal IgG to that on day −1. The vertical bars indicate the standard deviation.

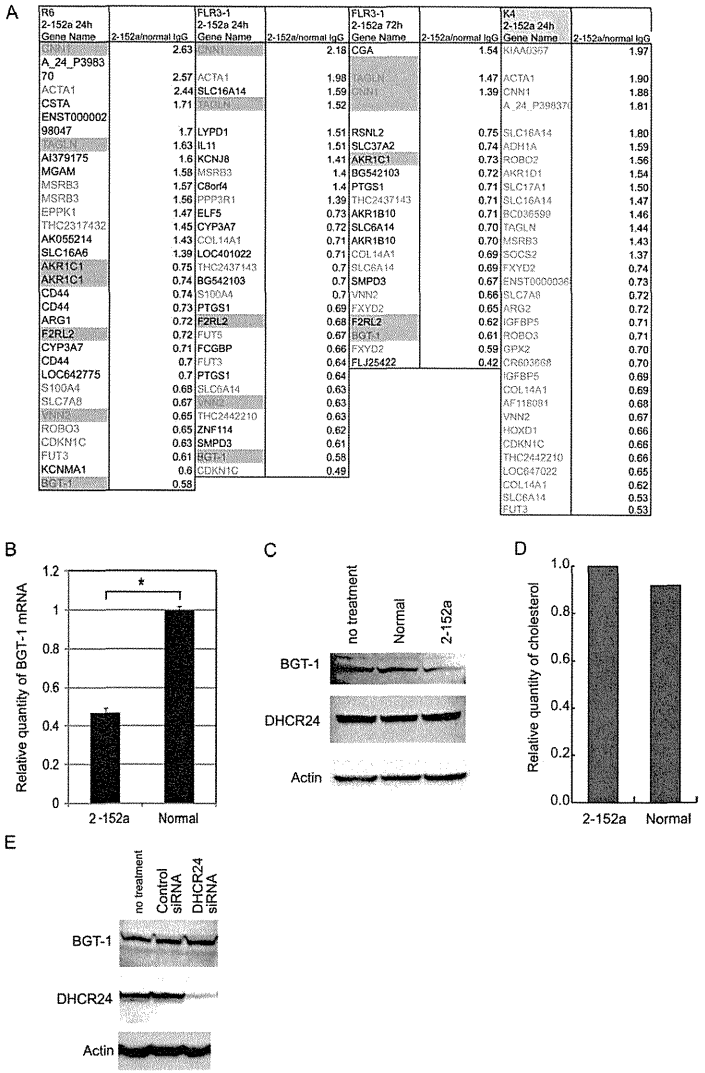

Figure 2. *A*, Genes that showed significant changes in expression after the 2-152a MAb treatment. HCV replicon cells (FLR3-1 and R6FLR-N) and K4 cells were treated with 2-152a MAb. The symbols shaded in gray indicate the genes that showed significantly changed expression commonly in R6FLR-N and FLR3-1 cells, and those shaded in orange indicate the genes that showed significantly changed expression in K4 cells. The amount of labeled probe for microarray analysis was 7-fold higher than that in the first experiment (Supplementary Table 1). Each value indicates the number of ratios of signal 2-152a MAb/normal IgG treatment. *B*, TaqMan expression assay of BGT-1 in samples of R6FLR-N cells treated with 2-152a MAb or normal IgG. BGT-1 mRNA (0.5 μg) samples treated with 2-152a MAb or normal IgG were transcribed by reverse transcriptase, and synthesized cDNAs were used for TaqMan

infected with HCV (Figure 1*D* and *F*). We detected viral protein (core) (Figure 1*B*) or viral RNA in cells (Figure 1*C*) and mouse blood by using RTD-PCR (Figure 1*D*). There was a significant reduction in the viral titers with 2-152a MAb treatment compared with that in normal IgG treatment (control) ($P < .005$, Figure 1*C* and *D*). No significant effects on body weight were observed by the inoculation of 2-152a MAb (Figure 1*E*). Further, no significant differences were found among the levels of human albumin in the sera of the normal IgG- and 2-152a MAb-inoculated mice (Figure 1*F*).

Expression of DHCR24 in Carcinoma Cells and on the Surface of HuH-7-Derived Cells

We observed abundant intracellular expression of DHCR24 in hepatoma cell lines in the previous study [12]; therefore, we characterized its expression on the surface of various carcinoma cell lines by flow cytometric analysis to clarify the mechanism of 2-152a MAb antiviral effects. In this analysis, DHCR24 expression was localized to the surface of the HuH-7 and HuH-7-based cell lines, HCV replicon cell lines (R6FLR-N, FLR3-1, and JFH-1), HCV persistently infected cell line (JFH/K4), and K4 cells; on the other hand, DHCR24 was not significantly expressed on the surface of the HepG2, Hep3B, RzM6-0d, RzM6-LC, WRL68, and PLC/PRF/5 cell lines (Supplementary Figure 1*C*). To confirm the expression of DHCR24 on the cell surface, we performed immunofluorescence staining (Supplementary Figure 1*D*). DHCR24 expression was detected in the HuH-7 cells without permeabilization.

Suppression of BGT-1 mRNA Expression in HCV Replicon Cell Lines After Treatment With 2-152a MAb

To determine the molecular mechanism underlying the effects of 2-152a MAb, we performed microarray analysis twice with different amounts of probes and evaluated the changes in gene expression associated with the 2-152a MAb treatment, which were specific to the HCV replicon cells rather than to the HCV-cured K4 cells. Using this methodology, we identified approximately 3–14 genes as upregulated and about 17–20 genes as downregulated following the treatment with 2-152a MAb, compared with the expressions in normal IgG-treated R6FLR-N, FLR3-1, and K4 cells (Figure 2*A*). Among these genes, the expression level of SLC6A12 (BGT-1; GenBank accession number NM_003044) showed significant downregulation in both the R6FLR-N and the FLR3-1 cell lines but not in the K4 cells (Figure 2*A*; Table 1). To validate this result, we tested BGT-1 mRNA expression in R6FLR-N cells treated with 2-152a MAb and normal IgG by using TaqMan expression assay. This assay demonstrated that the relative expression of BGT-1 was significantly suppressed by the treatment with 2-152a MAb ($P < .001$, Figure 2*B*). Significant downregulation of BGT-1 was also observed by treatment with 2-152a MAb in HCV-JFH-1-infected cells (Figure 2*C*).

We further addressed the mechanism of action of 2-152a MAb. Treatment with 2-152a MAb did not decrease the level of cholesterol (Figure 2*D*), and silencing of DHCR24 did not influence BGT-1 significantly (Figure 2*E*).

Inhibition of HCV Replication and Infection by siRNA Directed Against BGT-1

Because BGT-1 expression was suppressed by the treatment with 2-152a MAb, which had antiviral activity, we attempted BGT-1 silencing in HCV replicon cell lines by using designed siRNAs to examine the potential role of BGT-1 in HCV replication. BGT-1 silencing was confirmed by RT-PCR (Figure 3*A*). The effect of the siRNAs on HCV replication was examined by Western blotting with anti-NS5A antibody (Figure 3*B*) and measured by the luminescence level (Figure 3*C*, left panel) and cell viability (Figure 3*C*, right panel) in FLR3-1 cells. We also examined the effect of these siRNAs in R6FLR-N and JFH-1 cells (Supplementary Figure 2*A*) and observed similar inhibitory effects as those in FLR3-1 cells. The median inhibitory concentration (IC_{50}) values of BGT-1 siRNAs in various HCV replicon cell lines were as follows: FLR3-1 cells, 0.93 nM; R6FLR-N cells, 1.37 nM; JFH-1 cells, 5.95 nM. The cell viability was not significantly influenced by the siRNA treatment (Figure 3*C*, right panel; Supplementary Figure 2*A*, right panel).

Further, we monitored the levels of HCV RNA in JFH/K4 cells and their supernatants after BGT-1 silencing. Using RTD-PCR, we detected significant suppression in the HCV RNA levels by BGT-1 silencing in these cells ($P < .005$; Figure 3*D*, left panel) and their supernatants ($P < .05$; Figure 3*D*, right panel). These results were consistent with the strong inhibitory effects of

Table 1. Screened Genes in HCV Replicon Cell Lines After Treatment of IgG

	Gene name	R6FLR-N 24 hours	FLR3-1 24 hours	FLR3-1 72 hours	HuH-7/K4 24 hours
Screened specifically in replicon cells[a]					
1st screening	AKR1C1	0.67	0.62	0.65	NS
	BGT-1	0.53	0.63	0.53	NS
2nd screening	AKR1C1	0.74	NS	0.73	NS
(7-fold)[a]		or 0.75			
	F2RL2	0.72	0.68	0.62	NS
	BGT-1	0.58	0.58	0.61	NS
Screened in replicon and cured K4 cells[b]					
1st screening	CNN1	2.75	0.6	1.62	1.9
2nd screening	CNN1	2.63	2.18	1.39	1.88
(7-fold)[c]	TAGLN	1.63	1.52	1.47	1.44
	VNN2	0.65	0.63	0.66	0.67

Abbreviations: HCV, hepatitis C virus; IgG, immunoglobin G; NS, not screened.

[a] Screened genes were significantly changed in HCV replicon cells but not in HuH-7/K4 cells; each value indicates ratio of signal 2-152a MAb IgG/normal IgG treatment.

[b] Screened genes were significantly changed in all cell lines, including replicon cells and HuH-7/K4 cells.

[c] Comparing to 1st screening, 7-fold amount of labeled probe was used for microarray.

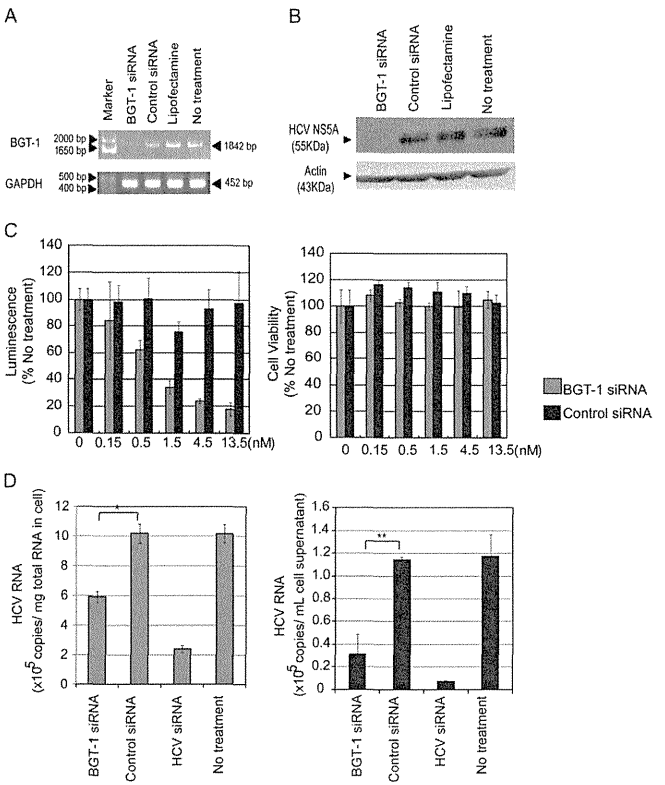

Figure 3. BGT-1 silencing by siRNA inhibits HCV replication in subgenomic HCV replicon cell lines and the persistently infected cell line. *A*, The siRNA targeting BGT-1 suppressed the expression of the corresponding mRNA. The mRNA of each sample was extracted 72 hours after siRNA (10 nM) transfection. Total RNA was transcribed and amplified by RT-PCR using primers specific to the open reading frame (ORF) of the BGT-1 (1842 bp) gene. The experiments were performed in triplicate, and the representative data are presented. *B*, The effects of BGT-1 siRNA (10 nM) on HCV were confirmed by Western blot analysis using an antibody against the HCV NS5A protein (55 kDa). The blots were striped and reprobed with an antibody directed against actin to examine protein loading in each lane. *C*, Levels of HCV replication (left panel) and cell viability (right panel) are presented according to serial concentrations of siRNA targeting BGT-1 and control siRNA in FLR3-1 cells (72 hours after transfection). The inhibition of replication or cell viability following siRNA targeting BGT-1 is defined relative to those of the cells that received no treatment (100%). The error bars represent the standard error of triplicate experiments. *D*, Quantification of HCV RNA by RTD-PCR in HCV persistently infected cells (JFH/K4) after treatment with BGT-1 siRNA. The cells were treated with siRNAs (10 nM) against BGT-1, control, and HCV (HCV R7) and harvested at 72 hours after transfection. TaqMan quantitative RT-PCR was performed for quantitation of HCV RNA in extracted RNA from cells (left panel) and their supernatants (right panel). The single asterisk (*) and double asterisk (**) indicate $P < .005$ and $P < .05$ against the control, respectively. The mean values from triplicate wells are indicated, and the vertical bars indicate the standard deviation.

Figure 2 continued. gene expression assay. Each value was compensated with values of glyceraldehyde 3-phosphate dehydrogenase (GAPDH) mRNA as the internal control and normal IgG. The asterisk indicates $P < .001$, and the vertical bars indicate the standard deviation. *C*, Level of BGT-1 and DHCR24 proteins detected in JFH/K4 cells after treatment with 2-152a or normal IgG (10 μg/mL). *D*, The relative cholesterol amount was measured in R6FLR-N cells treated with 2-152a or normal IgG (10 μg/mL). *E*, BGT-1 and DHCR24 proteins were detected in normal IgG- or 2-152a IgG-treated R6FLR-N cells.

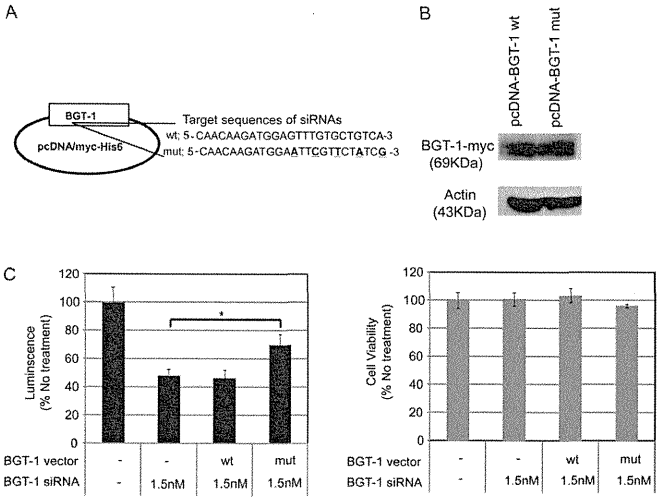

Figure 4. Validation of the inhibitory effects of BGT-1 siRNA on HCV replication in subgenomic HCV replicon cell lines. *A*, Schematic representation of the pcDNA-BGT-1 wild-type (wt) and mutant (mut) plasmids. The siRNA-targeted sites are indicated, and the underlined bold letters indicate the sequences induced by mutagenesis PCR. *B*, The wild type and mutant of the BGT-1-myc fusion protein were detected by using an anti-myc monoclonal antibody (9E10) in transfected R6FLR-N cells (upper panel). The blots were striped and reprobed with an antibody against actin to determine protein loading for each lane (lower panel). *C*, R6FLR-N cells were transfected with BGT-1 siRNA, and wild-type or mutant expression vectors were transfected after siRNA transfection. After 24 hours of vector transfection, the level of HCV replication (left panel) was measured by luminescence, and cell viability (right panel) was measured by WST-8 assay. The asterisk indicates $P < .05$ compared with transfection of siRNA alone. The mean values from triplicate wells are indicated, and the vertical bars represent the standard deviation.

BGT-1 siRNA on HCV replication, as shown in Figure 3*C*. We designed alternative siRNA targeting BGT-1 (BGT-1-siRNA-362) and observed its significant inhibitory effect on HCV replication without significant cytotoxicity (Supplementary Figure 2*B*).

Validation of the Anti-HCV Effects of siRNA Against BGT-1 by Rescue With Expression Vectors

To assess the specificity of BGT-1 silencing, we attempted to rescue HCV replication against the ectopic effects by this silencing. To examine the effect of the rescue, we constructed expression vectors of wild-type and mutant BGT-1 (Figure 4*A*) and confirmed the expression of each BGT-1-myc-fused protein (Figure 4*B*). The mutant BGT-1 vector contained 5 base mismatches within the site targeted by the BGT-1 siRNA without a change in the amino acid sequence of the protein (underlined in Figure 4*A*). We also transfected the pcDNA-BGT-1 plasmid after the siRNA treatment and observed significant recovery of HCV replication with mutant pcDNA-BGT-1 ($P < .05$; Figure 4*C*, left panel) without significant cytotoxicity (Figure 4*C*, right panel). BGT-1 expression was increased significantly in K4 cells in the presence of HCV ($P < .05$, Supplementary Figure 2*C*) at 72 hours after infection compared with the absence of HCV, and in RzM6-LC cells, which persistently express HCV [8], compared with RzM6-0d cells, which lack HCV expression ($P < .05$, Supplementary Figure 2*D*).

DISCUSSION

In this study, we determined that 2-152a MAb, which binds to but does not affect the activity of DHCR24, suppresses HCV replication and that BGT-1 is highly downregulated in HCV replicon cell lines treated with this antibody. Further, the efficient rescue of viral replication with a mutant expression vector indicates the specific inhibitory effect of BGT-1 silencing on HCV replication. Therefore, we hypothesize that BGT-1 plays an important role in HCV replication through a pathway that is likely independent of DHCR24, which in its own right can regulate the HCV life cycle [13].

BGT-1 is involved in sodium- and chloride-coupled betaine uptake, which helps in maintaining normal cellular conditions. Previous reports have described that the transcription of BGT-1 mRNA is regulated by a tonicity sensitive element (TonE) in response to hypertonic stress, a result that was first identified in the Madin-Darby canine kidney (MDCK) cell line [24]. BGT-1 is also thought to be responsible for the hyperosmotic stress response and in maintaining cell hydration. Denkert et al [25] reported that BGT-1 gene expression is induced by hyperosmolarity and inhibited by p38 mitogen-activated protein kinase ($p38^{MAPK}$) inhibitor SB20358. Further, several reports have evidenced that cell hydration affects viral replication and that viral replication increases during cell shrinkage due to hyperosmolarity, a result that was accompanied by increased BGT-1 mRNA expression [26]. Considering the reduction in HCV replication by the BGT-1 siRNA treatment, this treatment may prevent HCV replication by affecting hypoosmotic conditions in HCV-infected cells. Further studies are required to examine in detail the function of BGT-1 in HCV replication.

In summary, we demonstrated that the 2-152a monoclonal antibody inhibits HCV replication in HCV replicon cells and HCV infection in human hepatocytes transplanted into chimeric mice. The inhibitory effect of the monoclonal antibody on viral replication may be mediated by the suppression of BGT-1 expression. We propose BGT-1 as a key target for anti-HCV therapies.

Supplementary Data

Supplementary materials are available at *The Journal of Infectious Diseases* online (Supplementary Data).

Supplementary materials consist of data provided by the author that are published to benefit the reader. The posted materials are not copyedited. The contents of all supplementary data are the sole responsibility of the authors. Questions or messages regarding errors should be addressed to the author.

Notes

Acknowledgments. The authors thank I. Maruyama, K. Tanaka, T. Seki, and R. Takehara for their excellent technical support, and Y. Tokunaga for the insightful comments and helpful discussion.

Financial Support. This work was supported by grants from the Ministry of Health and Welfare of Japan; Ministry of Education, Culture, Sports, Science and Technology of Japan; Program for Promotion of Fundamental Studies in Health Sciences of the National Institute of Biomedical Innovation; and Cooperative Research Project on Clinical and Epidemiological Studies of Emerging and Reemerging Infectious Diseases.

Potential conflicts of interest. All authors: No reported conflicts.

All authors have submitted the ICMJE Form for Disclosure of Potential Conflicts of Interest. Conflicts that the editors consider relevant to the content of the manuscript have been disclosed.

References

1. Di Bisceglie AM, Carithers RL Jr, Gores GJ. Hepatocellular carcinoma. Hepatology **1998**; 28:1161–5.
2. Hayashi J, Aoki H, Arakawa Y, Hino O. Hepatitis C virus and hepatocarcinogenesis. Intervirology **1999**; 42:205–10.
3. Michielsen PP, Francque SM, van Dongen JL. Viral hepatitis and hepatocellular carcinoma. World J Surg Oncol **2005**; 3:27.
4. Mazzella G, Accogli E, Sottili S, et al. Alpha interferon treatment may prevent hepatocellular carcinoma in HCV-related liver cirrhosis. J Hepatol **1996**; 24:141–7.
5. Bruchfeld A, Stahle L, Andersson J, Schvarcz R. Ribavirin treatment in dialysis patients with chronic hepatitis C virus infection—a pilot study. J Viral Hepat **2001**; 8:287–92.
6. Kohara M, Tanaka T, Tsukiyama-Kohara K, et al. Hepatitis C virus genotypes 1 and 2 respond to interferon-alpha with different virologic kinetics. J Infect Dis **1995**; 172:934–8.
7. Nakamura H, Ogawa H, Kuroda T, et al. Interferon treatment for patients with chronic hepatitis C infected with high viral load of genotype 2 virus. Hepatogastroenterology **2002**; 49:1373–6.
8. Tsukiyama-Kohara K, Toné S, Maruyama I, et al. Activation of the CKI-CDK-Rb-E2F pathway in full genome hepatitis C virus-expressing cells. J Biol Chem **2004**; 279:14531–41.
9. Crameri A, Biondi E, Kuehnle K, et al. The role of seladin-1/DHCR24 in cholesterol biosynthesis, APP processing and Aβ generation in vivo. EMBO J **2006**; 25:432–43.
10. Waterham HR, Koster J, Romeijn GJ, et al. Mutations in the 3β-hydroxysterol Δ^{24}-reductase gene cause desmosterolosis, an autosomal recessive disorder of cholesterol biosynthesis. Am J Hum Genet **2001**; 69:685–94.
11. Lu X, Kambe F, Cao X, et al. 3β-Hydroxysteroid-Δ24 reductase is a hydrogen peroxide scavenger, protecting cells from oxidative stress-induced apoptosis. Endocrinology **2008**; 149:3267–73.
12. Nishimura T, Kohara M, Izumi K, et al. Hepatitis C virus impairs p53 via persistent overexpression of 3β-hydroxysterol Δ24-reductase. J Biol Chem **2009**; 284:36442–52.
13. Takano T, Tsukiyama-Kohara K, Hayashi M, et al. Augmentation of DHCR24 expression by hepatitis C virus infection facilitates viral replication in hepatocytes. J Hepatol **2011**; 55:512–21.
14. Lohmann V, Körner F, Koch J, Herian U, Theilmann L, Bartenschlager R. Replication of subgenomic hepatitis C virus RNAs in a hepatoma cell line. Science **1999**; 285:110–3.
15. Watanabe T, Sudoh M, Miyagishi M, et al. Intracellular-diced dsRNA has enhanced efficacy for silencing HCV RNA and overcomes variation in the viral genotype. Gene Ther **2006**; 13:883–92.
16. Sakamoto H, Okamoto K, Aoki M, et al. Host sphingolipid biosynthesis as a target for hepatitis C virus therapy. Nat Chem Biol **2005**; 1:333–7.
17. Kato T, Date T, Miyamoto M, et al. Efficient replication of the genotype 2a hepatitis C virus subgenomic replicon. Gastroenterology **2003**; 125: 1808–17.
18. Blight KJ, McKeating JA, Rice CM. Highly permissive cell lines for subgenomic and genomic hepatitis C virus RNA replication. J Virol **2002**; 76:13001–14.
19. Wakita T, Pietschmann T, Kato T, et al. Production of infectious hepatitis C virus in tissue culture from a cloned viral genome. Nat Med **2005**; 11:791–6.
20. Mercer DF, Schiller DE, Elliott JF, et al. Hepatitis C virus replication in mice with chimeric human livers. Nat Med **2001**; 7:927–33.
21. Inoue K, Umehara T, Ruegg UT, et al. Evaluation of a cyclophilin inhibitor in hepatitis C virus-infected chimeric mice in vivo. Hepatology **2007**; 45:921–8.
22. Takeuchi T, Katsume A, Tanaka T, et al. Real-time detection system for quantification of hepatitis C virus genome. Gastroenterology **1999**; 116:636–42.
23. Sarkar D, Imai T, Kambe F, et al. The human homolog of Diminuto/Dwarf1 gene (hDiminuto): a novel ACTH-responsive gene overexpressed in benign cortisol-producing adrenocortical adenomas. J Clin Endocrinol Metab **2001**; 86:5130–7.
24. Takenaka M, Preston AS, Kwon HM, Handler JS. The tonicity-sensitive element that mediates increased transcription of the betaine transporter gene in response to hypertonic stress. J Biol Chem **1994**; 269: 29379–81.
25. Denkert C, Warskulat U, Hensel F, Häussinger D. Osmolyte strategy in human monocytes and macrophages: involvement of p38MAPK in hyperosmotic induction of betaine and myoinositol transporters. Arch Biochem Biophys **1998**; 354:172–80.
26. Häussinger D. The role of cellular hydration in the regulation of cell function. Biochem J **1996**; 313:697–710.

Research Article

EASL EUROPEAN ASSOCIATION FOR THE STUDY OF THE LIVER | JOURNAL OF HEPATOLOGY

Augmentation of DHCR24 expression by hepatitis C virus infection facilitates viral replication in hepatocytes

Takashi Takano[1,†], Kyoko Tsukiyama-Kohara[2,*], Masahiro Hayashi[1], Yuichi Hirata[1], Masaaki Satoh[2], Yuko Tokunaga[1], Chise Tateno[3], Yukiko Hayashi[4], Tsunekazu Hishima[4], Nobuaki Funata[4], Masayuki Sudoh[5], Michinori Kohara[1]

[1]*Department of Microbiology and Cell Biology, Tokyo Metropolitan Institute of Medical Science, 2-1-6 Kamikitazawa, Setagaya-ku, Tokyo 156-8506, Japan;* [2]*Department of Experimental Phylaxiology, Faculty of Medical and Pharmaceutical Sciences, Kumamoto University, 1-1-1 Honjo, Kumamoto, Kumamoto 860-8556, Japan;* [3]*Phoenix Bio Co., Ltd., Study Service Department, 3-4-1 Kagamiyama, Higashi-Hiroshima 739-0046, Japan;* [4]*Department of Pathology, Tokyo Metropolitan Komagome Hospital, 3-18-22 Honkomagome, Bunkyo-ku, Tokyo 113-8677, Japan;* [5]*Kamakura Research Laboratories, Chugai Pharmaceutical Co., Ltd., Kajiwara 200, Kamakura-City, Kanagawa 247-8530, Japan*

Background & Aims: We characterized the role of 24-dehydrocholesterol reductase (DHCR24) in hepatitis C virus infection (HCV). DHCR24 is a cholesterol biosynthetic enzyme and cholesterol is a major component of lipid rafts, which is reported to play an important role in HCV replication. Therefore, we examined the potential of DHCR24 as a target for novel HCV therapeutic agents.
Methods: We examined DHCR24 expression in human hepatocytes in both the livers of HCV-infected patients and those of chimeric mice with human hepatocytes. We targeted *DHCR24* with siRNA and U18666A which is an inhibitor of both DHCR24 and cholesterol synthesis. We measured the level of HCV replication in these HCV replicon cell lines and HCV infected cells. U18666A was administrated into chimeric mice with humanized liver, and anti-viral effects were assessed.
Results: Expression of DHCR24 was induced by HCV infection in human hepatocytes *in vitro*, and in human hepatocytes of chimeric mouse liver. Silencing of *DHCR24* by siRNA decreased HCV replication in replicon cell lines and HCV JFH-1 strain-infected cells. Treatment with U18666A suppressed HCV replication in the replicon cell lines. Moreover, to evaluate the anti-viral effect of U18666A *in vivo*, we administrated U18666A with or without pegylated interferon to chimeric mice and observed an inhibitory effect of U18666A on HCV infection and a synergistic effect with interferon.
Conclusions: DHCR24 is an essential host factor which augmented its expression by HCV infection, and plays a significant role in HCV replication. DHCR24 may serve as a novel anti-HCV drug target.

Keywords: Hepatitis C virus; Replication; DHCR24; U18666A.
Received 18 April 2010; received in revised form 11 November 2010; accepted 2 December 2010; available online 22 December 2010
* Corresponding author. Address: Department of Experimental Phylaxiology, Faculty of Life Sciences, Kumamoto University, 1-1-1 Honjo, Kumamoto, Kumamoto 860-8556, Japan. Tel./fax: +81 96 373 5560.
E-mail address: kkohara@kumamoto-u.ac.jp (K. Tsukiyama-Kohara).
† Present address: Division of Veterinary Public Health, Nippon Veterinary and Life Science University, 1-7-1 Kyonan, Musashino, Tokyo 180-8602, Japan.
Abbreviations: DHCR24, 24-dehydrocholesterol reductase; HCV, hepatitis C virus; MoAb, monoclonal antibody; HCC, hepatocellular carcinoma; HBV, hepatitis B virus.

Introduction

Extensive epidemiological studies have identified multiple risk factors for hepatocellular carcinoma (HCC), including chronic infection with hepatitis C virus (HCV), and hepatitis B virus (HBV), and cirrhosis due to non-viral etiologies, such as alcohol abuse and aflatoxin B1 exposure [1,2]. Of these factors, HCV appears to be the dominant causative factor for HCC in many developed countries. The World Health Organization estimates that 170 million people worldwide are infected with HCV and are, therefore, at risk of developing liver cirrhosis and HCC [3]. The combination of pegylated interferon-α (PEG-IFN-α) and ribavirin is currently the standard treatment regimen for patients with chronic HCV infection. However, viral clearance is achieved in only 40% to 60% of patients and depends on the HCV genotype with which the patient is infected [4].

We previously established the RzM6 cell line, a HepG2 cell line in which the full-length HCV genome (HCR6-Rz) can be conditionally expressed under control of the Cre/*lox*P system and is precisely self-trimmed at the 5′ and 3′-termini by ribozyme sequences [5]. Anchorage-independent growth of these cells accelerates after 44 days of continuous passaging, during which the Cdk-Rb-E2F pathway is activated [5]. In a previous study, we developed monoclonal antibodies (MoAbs) against cell surface antigens on HCV-expressing cells that had been passaged for over 44 days [6]. One of the targets of these MoAbs was 24-dehydrocholesterol reductase (DHCR24 is also called 3-β-hydroxysterol-Δ-24-reductase, seladin-1, desmosterol delta-24-reductase), a molecule that is frequently overexpressed in the hepatocytes of HCV-infected patients.

DHCR24 confers resistance to apoptosis in neuronal cells [7]. It also regulates the cellular response to oxidative stress by binding to the amino terminus of p53, thereby displacing mouse double minute 2 homolog isoform MDM2 (*Homo sapiens*) (MDM2) from p53 and inducing the accumulation of p53 in human embryonic fibroblasts [8].

DHCR24 is a cholesterol biosynthetic enzyme that is also called desmosterol reductase [9,10]. Cholesterol is a major component of lipid rafts, which are reported to play an important role in HCV replication [11]. Therefore, we characterized the role of DHCR24 in HCV replication and evaluated its potential as a target for novel HCV therapeutic agents. We also examined the synergistic antiviral effect of U18666A which is an inhibitor of both DHCR24 [12] and cholesterol synthesis [13] with IFN-α in the treatment of HCV.

Materials and methods

Cells and plasmids

Cell culture methods of the HuH-7 [14], HepG2 [15], hybridoma and myeloma PAI cells, RzM6 cells [5], and the HCV subgenomic replicon cells lines FLR3-1 (genotype 1b, strain Con-1; [16]), R6FLR-N (genotype 1b, strain N; [17]), and Rep JFH Luc3-13) genotype 2a, strain JFH-1 [18]) were utilized to evaluate HCV replication [19] are described in Supplementary data.

The *DHCR24* cDNA was synthesized and amplified by PCR using Phusion™ DNA polymerase (Finnzymes) and cloned into the pcDNA3.1 vector (Invitrogen) or lentivirus vector, as described previously [6].

Matrix-assisted laser desorption ionization time-of-flight mass spectrometry analysis

The detailed procedures are described in Supplementary data [20].

Immunohistochemistry and Western blot analysis

The detailed procedures are described in Supplementary data.

The antibodies used in this experiment were: anti-Core, anti-NS3, anti-NS4B, anti-NS5B [5], and anti-NS5A (kindly provided by Dr. Matsuura, Osaka University), and anti-actin (Sigma).

Inhibition of DHCR24 by siRNA

We synthesized two siRNAs that were directed against human *DHCR24* mRNA: siDHCR24-417 and siDHCR24-1024. The target sequence of siDHCR24-417 was 5′-GUACAAGAAGACACACAAATT-3′, while that of siDHCR24-1024 was 5′-GAGAACUAUCUGAAGACAATT-3′. Additionally, we used siRNAs targeted against the HCV genome (siE-R7 and siE-R5) [17,21]. The siCONTROL Non-Targeting siRNA #3 (Dharmacon RNA Technologies) was used as the negative control siRNA. The chemically synthesized siRNAs were transfected into cells using Lipofectamine RNAiMAX (Invitrogen) and Opti-MEM (Invitrogen) by reverse-transfection. Cells were characterized 72 h after transfection.

Inhibition of viral replication by U18666A

U18666A (Calbiochem) was utilized to treat HCV replicon cells at a concentration of 62.5–1000 nM and chimeric mice at a concentration of 10 mg/kg (i.p.).

To determine whether cholesterol can reverse the U18666A treatment by the addition of cholesterol, we performed the experiments using HCV replicon cells (4×10^3 cells/well in a 96-well white plate, SUMILON). Culture medium was replaced after the cells had spread (at 24 h), and LDL (Calbiochem) was added to reach a final cholesterol concentration of 50 μg/ml. After a 24 h-incubation, U18666A (62.5, 125, 250, 500, and 1000 nM) was added to each well, and the cells were incubated for an additional 48 h. HCV replication activity was measured by luciferase assay, and cell viability was measured with the WST-8 cell counting kit according to the manufacturer's instructions (Dojindo Laboratories). Cholesterol measurements are described in Supplementary data.

Inhibition assay of HCV replication in replicon cells and persistent infected cells

For evaluation of the anti-HCV replication effect of the inhibitor U18666A in replicon cells and HCV persistently infected cells are described in Supplementary data.

Real-time detection (RTD)-PCR

Total RNA was purified from JFH-K4 cells that had been treated with siRNA or U18666A by the acid guanidium–phenol–chloroform method. HCV RNA was quantified by RTD-PCR as previously described [22].

HCV infection of chimeric mice with humanized liver and mRNA quantification by RTD-PCR

We used chimeric mice that were created by transplanting human primary hepatocytes into severe combined immunodeficient mice carrying a urokinase plasminogen activator transgene [23,24] that was controlled by the albumin promoter. These hepatocytes had been infected with plasma from a HCV-positive patient HCR6 (genotype 1b) [19]. The HCV 1b RNA level reached 2.9–18.0×10^6 copies/ml in mouse sera after 1–2 months of infection. HCV RNA in the mouse serum or total RNA from liver tissue from humanized chimeric mice with/without HCV infection was extracted using the acid guanidium–phenol–chloroform method. HCV RNA and *DHCR24* mRNA levels were quantified by RTD-PCR [22]. The primers and probes for HCV were prepared as previously described [22], and the primers and probes for *DHCR24* were prepared using Taq-Man® Gene Expression assays (Applied Biosystems) according to the manufacturer's instructions. PEG-IFNα-2a (Chugai) was administered subcutaneously at a concentration of 30 μg/kg, at day 1, 4, 8, and 11 (the amount of PEG-IFN-α administered to the chimeric mice was 20-fold relative to that used in humans), and U18666A was administered intraperitoneally at a concentration of 10 mg/kg, every day for 2 weeks (Fig. 6A). The protocols for the animal experiments were approved by the local ethics committee.

Human serum albumin in the blood of humanized chimeric mice was measured using a commercially available kit, according to the manufacturer's instructions (Alb-II kit; Eiken Chemical).

Results

Identification of DHCR24

We inoculated mice (BALB/c) with RzM6 cells that expressed HCV protein and had been cultured for over 44 days (denoted as RzM6-LC cells); mice were inoculated at least seven times over a 2-week period. We then fused the splenocytes from mice that had been immunized with RzM6-LC cells to myeloma cells to establish hybridomas. Characterization of the culture supernatant from more than 1000 hybridoma cells by ELISA (data not shown) revealed that one MoAb clone (2-152a) recognized a molecule of approximately 60 kDa in various cells (Supplementary Fig. 1A and B. This molecule was more highly expressed in RzM6-LC cells (Supplementary Fig. 1A), HeLa cells, and HCC cell lines (HepG2, HuH-7, Hep3B, and PLC/PRF/5) than in HEK293 cells and several normal liver cell lines (NKNT, TTNT, and WRL68) (Supplementary Fig. 1B). To further characterize this molecule, we performed matrix-assisted laser desorption ionization time-of-flight mass spectrometry (MALDI-TOF-MS) and obtained seven peptide sequences (Supplementary Fig. 1C, underlined). These peptide sequences suggested that the molecule that was recognized by the 2-152a antibody was DHCR24. We constructed a lentivirus expression vector containing myc-tagged DHCR24 (DHCR24-myc) and transduced it into HepG2 cells. By western blot analysis with 2-152a and anti-Myc antibody, we then confirmed that DHCR24 was expressed in the transduced cells (Supplementary Fig. 1D). We found that the 2-152a antibody specifically recognized DHCR24.

Author's personal copy

Viral Hepatitis

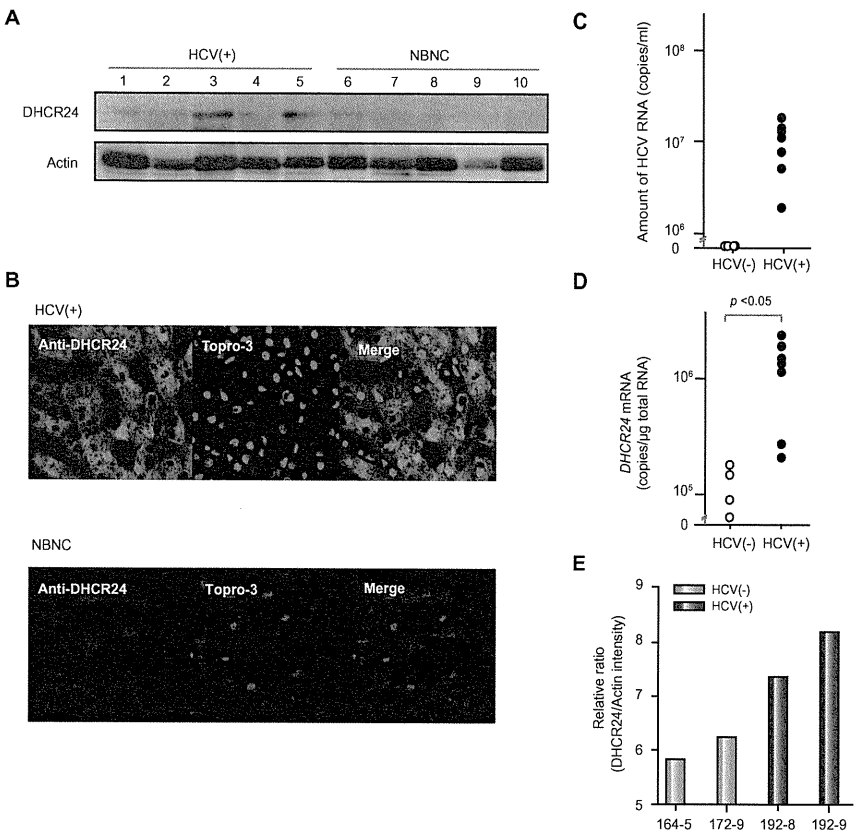

Fig. 1. HCV induces DHCR24 overexpression *in vitro* and *in vivo*. (A) Expression of DHCR24 in non-cancerous regions of livers of HCV-infected (+) and NBNC-HCC patients. Lysates (25 μg/lane) of non-cancerous liver tissues from HCC patients were analyzed by Western blot analysis using MoAb 2-152a. The patient numbers (Supplementary Table 1) are indicated at the top of the blot. (B) Immunohistochemical staining of HCV-infected non-cancerous tissues derived from an HCC patient using the monoclonal antibody 2-152a (Alexa488), anti-TO-PRO-3, or a merge (600× magnification) (upper panel). Tissues from an NBNC patient stained with the monoclonal antibody 2-152a (Alexa488) as well as TO-PRO-3 (640× magnification) (lower panel). (C) The amount of HCV RNA that was present in the HCV-R6 (genotype 1b)-infected chimeric mice with the humanized liver was quantified using RTD-PCR. The results of HCV uninfected ($n = 4$) and infected ($n = 7$) is indicated. (D) The amount of *DHCR24* mRNA present in total RNA isolates of HCV-R6 (genotype 1b)-infected chimeric mice with the humanized liver was quantified using RTD-PCR. *$p < 0.05$ (Mann–Whitney test). The results of HCV uninfected ($n = 4$) and infected ($n = 7$) are indicated. (E) DHCR24 protein was detected by Western blot analysis using MoAb 2-152a as a probe, and quantitated by LAS3000. Protein levels are normalized to actin and ratio is indicated.

HCV infection in vivo induces persistent overexpression of DHCR24

We next examined whether HCV infection could induce DHCR24 expression in human hepatocytes. DHCR24 was overexpressed more frequently in liver tissues from HCV-positive patients than in tissues from HBV- and HCV-negative (NBNC) patients (Fig. 1A and Supplementary Table 1). The liver tissue from HCV-positive patients stained more strongly for DHCR24 expression than the liver tissue from NBNC patients (Fig. 1B). We inoculated chimeric mice [19,23,25] with HCV ($10^{6.2}$ copies/ml) that had been isolated from the plasma of HCV-infected patients (patient R6, HCV genotype 1b). The serum concentration of human albumin (Supplementary Fig. 2A) in the chimeric mice after transplantation of hepatocytes indicated that human hepatocytes had engrafted in the mouse livers. Thirty days after transplantation, mice were infected with HCV, and HCV and RNA titers were analyzed both before and after inoculation (Supplementary Fig. 2B). The average amount of HCV RNA that was present in the serum of the infected chimeric mice at 28 days post-infection was 1.1×10^7 copies/ml (Fig. 1C and Supplementary Fig. 2B). The *DHCR24* mRNA levels in the livers of the chimeric mice were also quantified at 28 days post-infection by real-time detection (RTD)-PCR [22]. The results revealed that there was a significant increase in *DHCR24* expression as measured by mRNA levels in HCV infected chimeric mice (Fig. 1D). Next, we examined the extent to which translation of DHCR24 occurred in the chimeric mice (Fig. 1E), higher DHCR24 protein levels were present in hepatocytes from HCV-infected mice (Nos. 192-8 and 192-9) than in those of uninfected mice (Nos. 164-5 and 172-9). These findings indicate that expression of DHCR24 is significantly up-regulated by HCV infection in human hepatocytes.

Role of DHCR24 in HCV replication

Since augmentation of DHCR24 expression was observed by HCV infection in humanized chimeric mice, we next examined whether DHCR24 was involved in HCV replication or not. We transfected siRNA into HCV replicon cell lines FLR3-1 (Fig. 2A and B) and R6FLR-N (Fig. 2C and D). Treatment with either two different *DHCR24* siRNA molecules (siDHCR24-417 or -1024) decreased HCV replication in a dose-dependent manner (Fig. 2A and C) but did not appear to have a significant effect on cell viability (Fig. 2B and D). Western blot analysis using HCV subgenomic replicon cell lines confirmed these findings (Fig. 2E and F). We also transfected the *DHCR24* siRNAs into HCV JFH-1 strain [18]-infected HuH7/K4 cell lines and found, by Western blot analysis, that the siRNAs inhibited HCV protein expression (Fig. 2G and H). These results indicate that DHCR24 may play a role in HCV replication.

The expression level of DHCR24 is linked to intracellular cholesterol levels

Human DHCR24 is involved in cholesterol biosynthesis [10]. It participates in multiple steps of cholesterol synthesis from lanosterol [26] (Fig. 3A). To examine the effect of cholesterol on the DHCR24 expression level in HuH-7 cells, we added cholesterol to cultured cells and determined the DHCR24 expression level (Fig. 3B). Expression levels of DHCR24 in HuH-7 cells were decreased approximately 50% by addition of cholesterol compared to that of the untreated control (Fig. 3B). On the other hand, that of DHCR24 in HepG2 cells was increased 2.5-fold by depletion of cholesterol using methyl-β-cyclodextrin (M-β-CD) (Fig. 3C).

These results indicate that the expression of DHCR24 in a cell correlates with the cholesterol level in that cell. Furthermore, silencing *DHCR24* reduced the cholesterol level in cells compared to control cells (Fig. 3D), suggesting that DHCR24 is essential for cholesterol synthesis.

Effect of U18666A on HCV replication in vitro

We further examined the role that DHCR24 plays in HCV replication by treating cells with U18666A. Treatment with U18666A (62.5, 125, 250, 500, and 1000 nM) of HCV replicon cells (FLR3-1) decreased HCV replication in a dose-dependent manner as shown by luciferase assay (Fig. 4A) and Western blot analysis (Fig. 4B). Notably, DHCR24 protein appeared as doublet bands in the absence of U18666A, but the lower band shifted to the upper band after treatment with U18666A (Fig. 4B). U18666A also suppressed HCV replication in other replicon cell lines (R6FLR-N and Rep JFH Luc 3-13; Fig. 4C and D). Treatment with U18666A (<250 nM) suppressed viral replication without producing significant cytotoxicity. We also examined the effect of 7-dehydrocholesterol reductase (DHCR7) (Fig. 3A) on HCV replication using the specific inhibitor BD1008 [26]. Treatment with BD1008 also suppressed HCV replication, but the concentration required was much higher than that needed in the U18666A assays (Fig. 4E); the concentration also greatly exceeded the intrinsic IC_{50} value for inhibition of σ-receptor binding (47 ± 2 nM) [27]. Therefore, DHCR24 may play a more significant role than DHCR7 in HCV replication. We next evaluated the compensatory effect that the addition of cholesterol had on cells treated with U18666A (Fig. 4F and G) by examining low density lipoprotein (LDL)-replaceable dissolved cholesterol levels as described in Supplementary data. Treatment with cholesterol led to partial restoration of HCV replication (Fig. 4F). These results suggest that U18666A suppresses HCV replication by depleting cellular cholesterol stores.

Next, we characterized the effect that U18666A had on HCV JFH-1 infection. Adding U18666A (62.5, 125, 250, and 500 nM) to HCV JFH-1-infected cell lines for 72 h, reductions of NS5B protein level were observed in cells treated more than 500 nM of U18666A (Fig. 5A and B). Additionally, the HCV RNA copy number in infected cells was suppressed by addition of 250 or 500 nM of U18666A (Fig. 5C). Examination of the cytotoxicity that U18666A (62.5–500 nM) had on infected cells revealed that it had little effect on cell viability (Fig. 5D). These results demonstrate that inhibition of DHCR24 by U18666A suppresses viral replication in HCV replicon cells and HCV-infected cells.

Evaluation of the anti-HCV effect of U18666A in vivo

To examine the effect of U18666A on HCV infection *in vivo*, we administered U18666A to HCV-infected chimeric mice with the humanized liver. The mice were infected with HCV via inoculation of patient serum HCR6 5 weeks after transplantation of human hepatocytes. U18666A (10 mg/kg) and PEG-IFN-α (30 μg/kg) were then administrated to these mice for 2 weeks (Fig. 6A). HCV RNA quantity (Fig. 6B) and serum human albumin levels (Fig. 6C) were measured in the mice after 1, 4, and 14 days of HCV infection. Treatment with U18666A alone significantly decreased HCV RNA levels in the serum (from 1×10^8 to 3×10^5 copies/ml) after 2 weeks, and its suppressive effect was more pronounced than that of PEG-IFN-α alone (8×10^5 copies/ml; Fig. 6B). Moreover, co-administration of U18666A and PEG-IFN-α synergistically (combination index <1) enhanced the anti-viral effect of PEG-IFN-α (5×10^4 copies/ml). Treatment with these drugs did not significantly affect the serum human albumin concentrations in treated mice (Fig. 6C).

Discussion

The results of this study revealed that DHCR24, an enzyme that participates in cholesterol synthesis (last step; Fig. 3A), also plays a significant role in HCV replication. To our knowledge, this is the first report that this molecule is involved in HCV infection. The mevalonate route of the cholesterol synthesis pathway (starting from acetyl Co-A) has previously been reported to be involved in

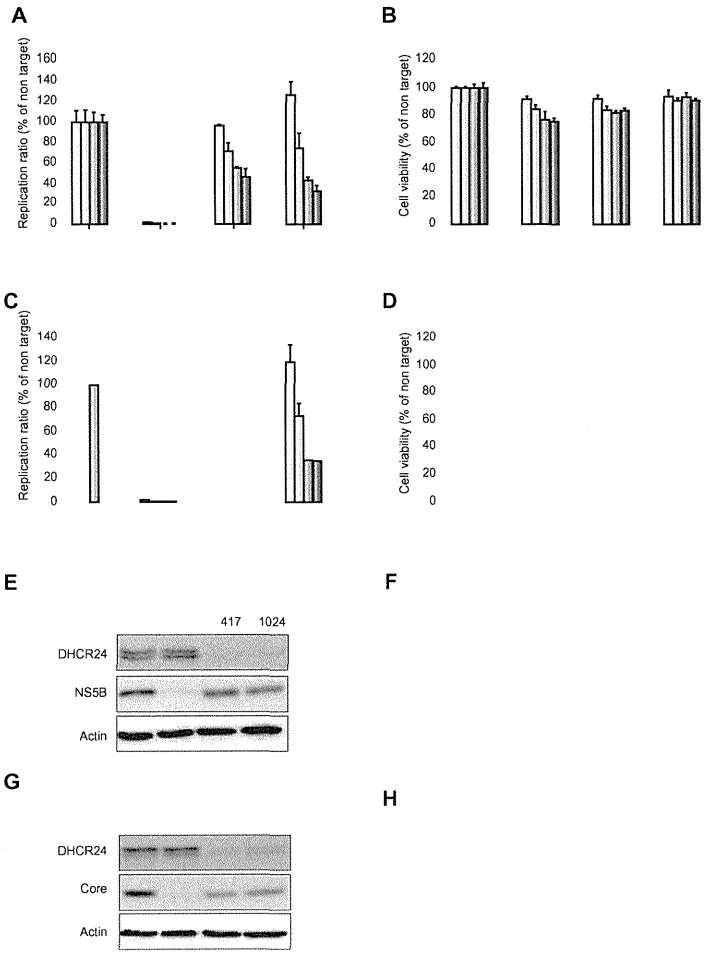

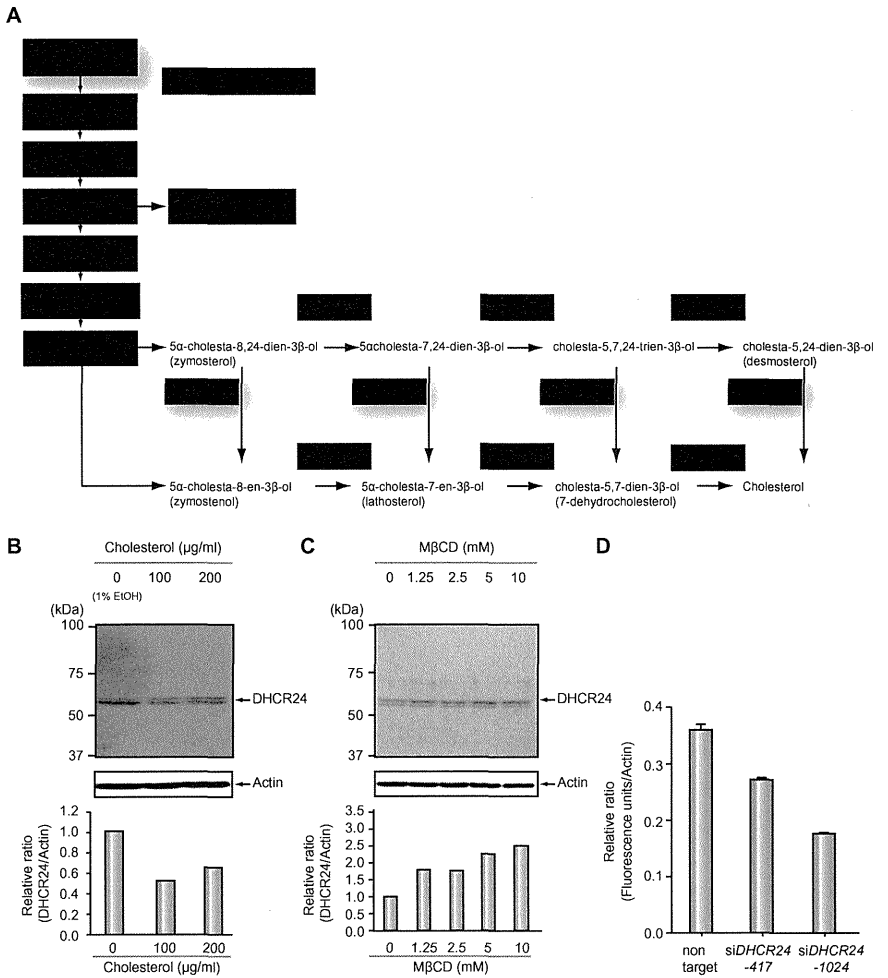

Fig. 3. The level of cholesterol and DHCR24 expression. (A) Cholesterol synthesis pathway, starting from HMG-CoA [26]. The abbreviations used are: D8D7I, 3β-hydroxysterol-delta(8)-delta(7)-isomerase; and C5DS, 3β-hydroxysterol-C^5-desaturase. (B) Cholesterol (0, 100, and 200 μg/ml) was added to HuH-7 cells, and, after 24 h, DHCR24 protein was detected by Western blot analysis using anti-DHCR24 MoAb and protein band intensity was measured and normalized to actin (lower panel). (C) HepG2 cells were treated with MβCD (0, 1.25, 2.5, 5, and 10 mM) for 30 min. After 72 h, these cells were harvested and examined by Western blot analysis with the anti-DHCR24 MoAb and relative intensity was measured as described in (B) (lower panel). (D) Cholesterol concentration in R6FLR-N cells was measured after treatment with non-targeting siRNA and *DHCR24* siRNA (417 and 1024). The cholesterol contents were measured by Amplex Red cholesterol assay, plotted based on fluorescence units and normalized to actin which was measured by Western blot analysis, and the relative ratio was then calculated. The data represent the mean of three experiments, and the bars indicate the SD values.

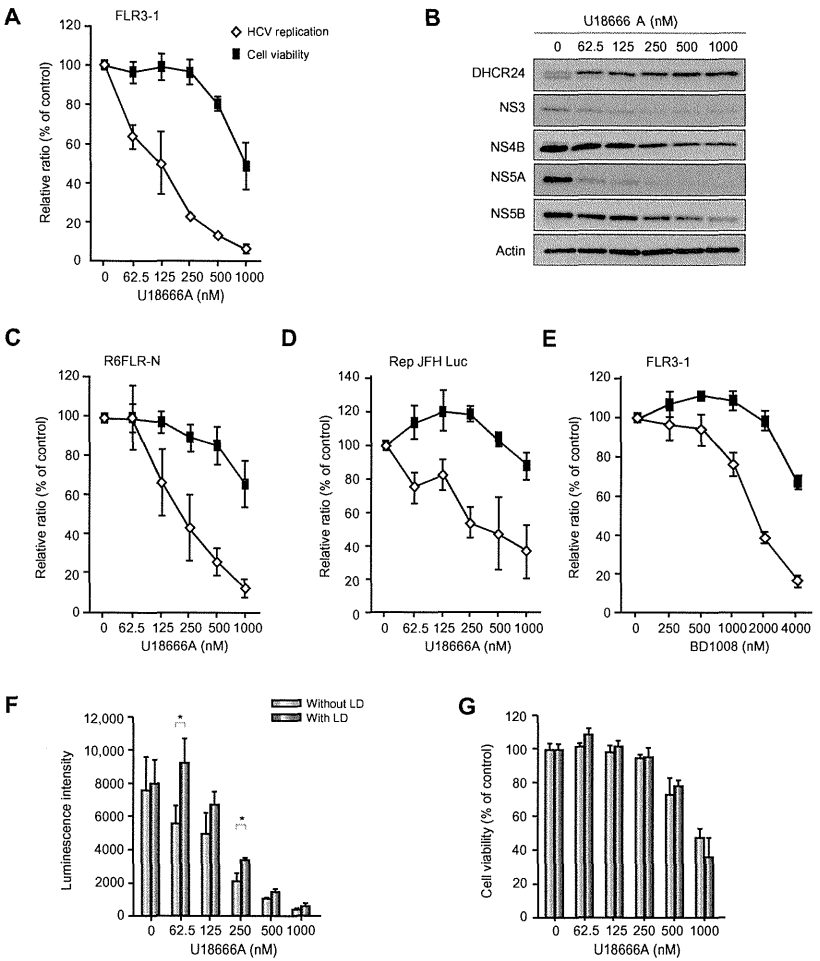

Fig. 4. Effect of U18666A on HCV replication. (A) Addition of U18666A to FLR3-1 cells and subsequent examination of HCV replication by the luciferase assay. Cell viability was measured by WST-8 assay. HCV replication and cell viability were measured 48 h after addition of U18666A. The bars indicate SD values. Open diamonds indicate the relative ratio of viral replication, and black squares indicate the cell viability in relation to untreated controls (A and C–E). (B) Treatment of FLR3-1 cells with U18666A decreased the expression of HCV proteins in a dose-dependent manner, as determined by Western blot analysis. (C and D) Effect of U18666A on HCV replication in other HCV replicon cells (C, R6FLR-N cells; D, Rep JFH Luc 3-13 cells). HCV replication and cell viability analyses were performed as described above. (E) The effect of the DHCR7 inhibitor BD1008 on HCV replicon cells (FLR3-1). Replication activity was examined by the luciferase assay, and cell viability was measured by the WST-8 assay. HCV replication and cell viability analyses were performed 48 h after the addition of U18666A. (F and G) FLR3-1 cells (5×10^3 cells/well) were treated with U18666A alone (light blue, or), low density lipoprotein (LDL) (final cholesterol concentration, 50 μg/ml), and U18666A (dark blue). HCV replication was determined by the luciferase assay 48 h later (F), and cell viability was measured by the WST-8 assay (G). *p <0.05 (two-tailed Student's t-test). The data represent the mean of three experiments, and the bars indicate SD values.

Author's personal copy

Viral Hepatitis

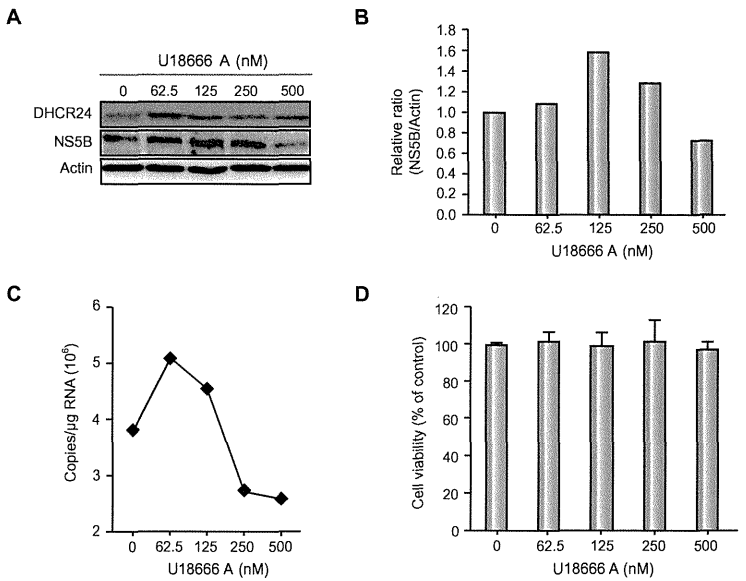

Fig. 5. Effect of U18666A on cells infected with HCV JFH-1. HCV JFH-1-infected cells treated with U18666A were examined 72 h after treatment. (A) Expression of HCV-NS5B protein with or without U18666A treatment, analyzed by Western blot analysis. (B) The intensity of HCV-NS5B protein expression is represented graphically. (C) HCV RNA in HCV JFH-1-infected cells with or without U18666A treatment was measured by RTD-PCR as described in Materials and methods. (D) Cell viability was measured by the WST-8 assay.

HCV replication [28]. The present findings are the first evidence that overexpression of one of the enzymes downstream of the mevalonate pathway, i.e., DHCR24, can be induced by HCV infection. In a previous study, 3-hydroxy 3-methyl-glutaryl Co-A (HMG-CoA) reductase was found to be inhibited by lovastatin, subsequently resulting in suppression of HCV replication [28]. The product of the mevalonate pathway that is required for HCV replication is reported to be a geranyl geranyl lipid [29]. Many lipids are crucial to the viral life cycle, and inhibitors of the cholesterol/fatty acid biosynthetic pathway inhibit viral replication, maturation, and secretion [30,31]. We found that inhibition of DHCR24 down-regulated HCV replication. DHCR24 catalyzes the reduction of the delta-24 bond of the sterol intermediate and works further downstream of farnesyl pyrophosphate (Fig. 3A) and, therefore, does not influence geranyl–geranylation. Thus, our findings indicate the existence of regulatory pathway of HCV replication by cholesterol synthesis and trafficking through DHCR24 rather than by protein geranyl–geranylation. DHCR24 deficiency reduces the cholesterol level and disorganizes cholesterol-rich detergent-resistant membrane domains (DRMs) in mouse brains [32]. Additionally, the HCV replication complex has been detected in the DRM fraction [11]. Therefore, a deficiency in DRM, induced by silencing *DHCR24*, may suppress HCV replication.

We demonstrated that the addition of cholesterol to HCV-infected hepatocytes treated with U18666A led to partial recovery of HCV replication, which suggests that cholesterol may be an important factor in HCV replication. U18666A impairs the intracellular biosynthesis and transport of cholesterol and inhibits the action of membrane-bound enzymes, including DHCR24, during sterol synthesis [33]. Moreover, the DHCR7 inhibitor BD1008 also suppresses HCV replication. Thus, the findings in this study further substantiate the fact that cholesterol plays an important role in HCV replication and infection.

Although monotherapy with statins is reportedly insufficient to induce anti-viral activity in HCV-infected patients [34], a synergistic action between statins and IFN has been observed [35]. The effect of the statin is thought to be mainly mediated by the depletion of geranyl geranyl lipids. It is important to note that higher doses of statins may increase the risk of myopathy, liver dysfunction, and cardiovascular events [36]. Moreover, the EC_{50} values of the statins that are associated with a reduction in HCV replication are reported to be 0.45–2.16 μM, while the IC_{50} of U18666A was estimated to be 125 nM in the present study. Therefore, U18666A may serve as a novel anti-HCV drug that could be utilized with IFN as a combined therapeutic regimen.

In summary, we demonstrated that the expression of DHCR24 is induced by infection with HCV and that DHCR24 is an essential host factor that is required for HCV replication. HCV may increase cholesterol synthesis in cells via the action of a host regulatory factor, such as DHCR24, that is correlated with cholesterol

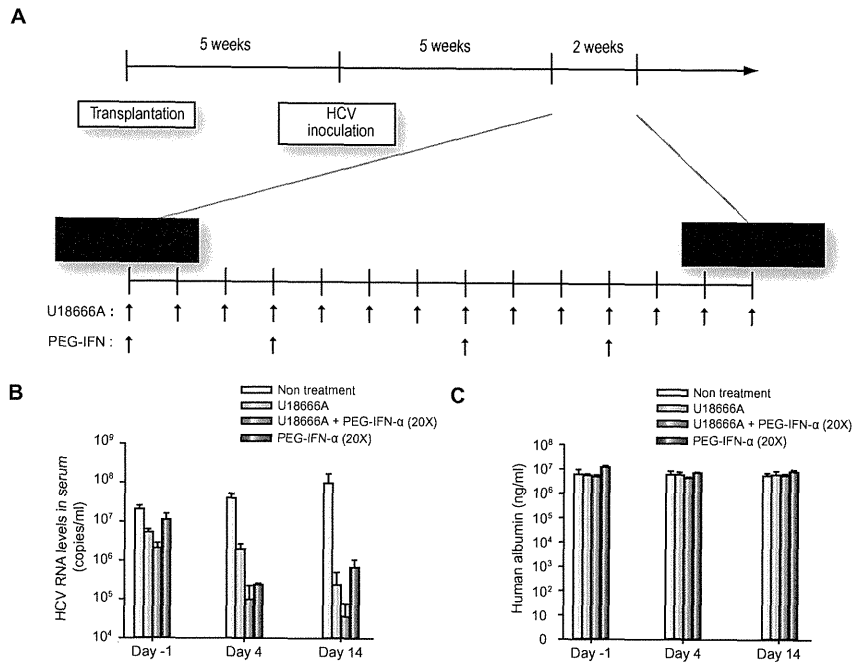

Fig. 6. Evaluation of the anti-HCV effect of U18666A in chimeric mice. (A) Diagram of the schedule that was followed to produce chimeric mice with the humanized liver, perform blood sampling, and administer drugs to chimeric mice infected with HCV. Four groups of three chimeric mice with the humanized liver were treated intraperitoneally with U18666A (10 mg/kg) and/or subcutaneously with PEG-IFN-α (30 μg/kg) at 2-day intervals for 2 weeks. (B) The effect of U18666A and/or PEG-IFN-α on HCV replication in chimeric mice with the humanized liver was determined by quantification of HCV-RNA using RTD-PCR. The bars indicate SD values ($n = 12$). (C) Human albumin concentrations in the sera of chimeric mice with the humanized liver. The bars indicate SD values ($n = 12$).

synthesis and is also directly involved in replication. Genome-wide analysis of the host response to HCV infection revealed the upregulation of genes related to lipid metabolism [37]. DHCR24 expression was found to be upregulated in the cDNA microarray analysis of chronic hepatitis C cases [38]. Future studies are needed to examine the detailed mechanism by which HCV infection augments DHCR24 expression in hepatocytes.

Conflict of interest

The authors who have taken part in this study declared that they do not have anything to disclose regarding funding or conflict of interest with respect to this manuscript.

Financial support

This study was supported in part by a grant from the Ministry of Education, Culture, Sports, Science and Technology of Japan, a grant from the Ministry of Health, Labor and Welfare of Japan, and the Program for Promotion of Fundamental Studies in Health Sciences of the National Institute of Biomedical Innovation of Japan and the Cooperative Research Project on Clinical and Epidemiological Studies of Emerging and Re-emerging Infectious Diseases.

Acknowledgments

We are very grateful to Dr. T. Watanabe, Dr. S. Nakagawa, Mr. T. Nishimura and Dr. K. Tanaka for technical support, and Dr. S. To'ne, Dr. T. Wakita, Dr. S. Sekiguchi, and Dr. F. Yasui for helpful discussions.

Supplementary data

Supplementary data associated with this article can be found, in the online version, at doi:10.1016/j.jhep.2010.12.011.

Author's personal copy

Viral Hepatitis

References

[1] Llovet JM, Burroughs A, Bruix J. Hepatocellular carcinoma. Lancet 2003;362:1907–1917.
[2] Tsukuma H, Hiyama T, Tanaka S, et al. Risk factors for hepatocellular carcinoma among patients with chronic liver disease. N Engl J Med 1993;328:1797–1801.
[3] Wasley A, Alter MJ. Epidemiology of hepatitis C: geographic differences and temporal trends. Semin Liver Dis 2000;20:1–16.
[4] Kohara M, Tanaka T, Tsukiyama-Kohara K, et al. Hepatitis C virus genotypes 1 and 2 respond to interferon-alpha with different virologic kinetics. J Infect Dis 1995;172:934–938.
[5] Tsukiyama-Kohara K, Tone S, Maruyama I, et al. Activation of the CKI-CDK-Rb-E2F pathway in full genome hepatitis C virus-expressing cells. J Biol Chem 2004;279:14531–14541.
[6] Nishimura T, Kohara M, Izumi K, et al. Hepatitis C virus impairs p53 via persistent overexpression of 3beta-hydroxysterol Delta24-reductase. J Biol Chem 2009;284:36442–36452.
[7] Greeve I, Hermans-Borgmeyer I, Brellinger C, et al. The human DIMINUTO/DWARF1 homolog seladin-1 confers resistance to Alzheimer's disease-associated neurodegeneration and oxidative stress. J Neurosci 2000;20:7345–7352.
[8] Wu C, Miloslavskaya I, Demontis S, Maestro R, Galaktionov K. Regulation of cellular response to oncogenic and oxidative stress by Seladin-1. Nature 2004;432:640–645.
[9] Waterham HR, Koster J, Romeijn GJ, et al. Mutations in the 3beta-hydroxysterol Delta24-reductase gene cause desmosterolosis, an autosomal recessive disorder of cholesterol biosynthesis. Am J Hum Genet 2001;69:685–694.
[10] Wechsler A, Brafman A, Shafir M, et al. Generation of viable cholesterol-free mice. Science 2003;302:2087.
[11] Aizaki H, Lee KJ, Sung VM, Ishiko H, Lai MM. Characterization of the hepatitis C virus RNA replication complex associated with lipid rafts. Virology 2004;324:450–461.
[12] Di Stasi D, Vallacchi V, Campi V, et al. DHCR24 gene expression is upregulated in melanoma metastases and associated to resistance to oxidative stress-induced apoptosis. Int J Cancer 2005;115:224–230.
[13] Bierkamper GG, Cenedella RJ. Induction of chronic epileptiform activity in the rat by an inhibitor of cholesterol synthesis, U18666A. Brain Res 1978;150:343–351.
[14] Nakabayashi H, Taketa K, Miyano K, Yamane T, Sato J. Growth of human hepatoma cells lines with differentiated functions in chemically defined medium. Cancer Res 1982;42:3858–3863.
[15] Knowles BB, Howe CC, Aden DP. Human hepatocellular carcinoma cell lines secrete the major plasma proteins and hepatitis B surface antigen. Science (New York, NY) 1980;209:497–499.
[16] Sakamoto H, Okamoto K, Aoki M, et al. Host sphingolipid biosynthesis as a target for hepatitis C virus therapy. Nat Chem Biol 2005;1:333–337.
[17] Watanabe T, Sudoh M, Miyagishi M, et al. Intracellular-diced dsRNA has enhanced efficacy for silencing HCV RNA and overcomes variation in the viral genotype. Gene Ther 2006;13:883–892.
[18] Wakita T, Pietschmann T, Kato T, et al. Production of infectious hepatitis C virus in tissue culture from a cloned viral genome. Nat Med 2005;11:791–796.
[19] Inoue K, Umehara T, Ruegg UT, et al. Evaluation of a cyclophilin inhibitor in hepatitis C virus-infected chimeric mice in vivo. Hepatology 2007;45:921–928.
[20] Jensen ON, Wilm M, Shevchenko A, Mann M. Sample preparation methods for mass spectrometric peptide mapping directly from 2-DE gels. Methods Mol Biol (Clifton, NJ) 1999;112:513–530.
[21] Nakagawa S, Umehara T, Matsuda C, et al. Hsp90 inhibitors suppress HCV replication in replicon cells and humanized liver mice. Biochem Biophys Res Commun 2007;353:882–888.
[22] Takeuchi T, Katsume A, Tanaka T, et al. Real-time detection system for quantification of hepatitis C virus genome. Gastroenterology 1999;116:636–642.
[23] Mercer DF, Schiller DE, Elliott JF, et al. Hepatitis C virus replication in mice with chimeric human livers. Nat Med 2001;7:927–933.
[24] Tateno C, Yoshizane Y, Saito N, et al. Near completely humanized liver in mice shows human-type metabolic responses to drugs. Am J Pathol 2004;165:901–912.
[25] Umehara T, Sudoh M, Yasui F, et al. Serine palmitoyltransferase inhibitor suppresses HCV replication in a mouse model. Biochem Biophys Res Commun 2006;346:67–73.
[26] Kedjouar B, de Medina P, Oulad-Abdelghani M, et al. Molecular characterization of the microsomal tamoxifen binding site. J Biol Chem 2004;279:34048–34061.
[27] John CS, Lim BB, Geyer BC, Vilner BJ, Bowen WD. 99mTc-labeled sigma-receptor-binding complex: synthesis, characterization, and specific binding to human ductal breast carcinoma (T47D) cells. Bioconjug Chem 1997;8:304–309.
[28] Ye J, Wang C, Sumpter Jr R, et al. Disruption of hepatitis C virus RNA replication through inhibition of host protein geranyl-geranylation. Proc Natl Acad Sci USA 2003;100:15865–15870.
[29] Kapadia SB, Chisari FV. Hepatitis C virus RNA replication is regulated by host geranyl-geranylation and fatty acids. Proc Natl Acad Sci USA 2005;102:2561–2566.
[30] Aizaki H, Morikawa K, Fukasawa M, et al. Critical role of virion-associated cholesterol and sphingolipid in hepatitis C virus infection. J Virol 2008;82:5715–5724.
[31] Syed GH, Amako Y, Siddiqui A. Hepatitis C virus hijacks host lipid metabolism. Trends Endocrinol Metab 2010;21:33–40.
[32] Crameri A, Biondi E, Kuehnle K, et al. The role of seladin-1/DHCR24 in cholesterol biosynthesis, APP processing and Abeta generation in vivo. EMBO J 2006;25:432–443.
[33] Cenedella RJ. Cholesterol synthesis inhibitor U18666A and the role of sterol metabolism and trafficking in numerous pathophysiological processes. Lipids 2009;44:477–487.
[34] Bader T, Fazili J, Madhoun M, et al. Fluvastatin inhibits hepatitis C replication in humans. Am J Gastroenterol 2008;103:1383–1389.
[35] Ikeda M, Abe K, Yamada M, et al. Different anti-HCV profiles of statins and their potential for combination therapy with interferon. Hepatology (Baltimore, MD) 2006;44:117–125.
[36] Argo CK, Loria P, Caldwell SH, Lonardo A. Statins in liver disease: a molehill, an iceberg, or neither? Hepatology (Baltimore, MD) 2008;48:662–669.
[37] Su AI, Pezacki JP, Wodicka L, et al. Genomic analysis of the host response to hepatitis C virus infection. Proc Natl Acad Sci USA 2002;99:15669–15674.
[38] Honda M, Yamashita T, Ueda T, et al. Different signaling pathways in the livers of patients with chronic hepatitis B or chronic hepatitis C. Hepatology 2006;44:1122–1138.

Journal of Medical Virology 83:801–809 (2011)

Translocase of Outer Mitochondrial Membrane 70 Expression Is Induced by Hepatitis C Virus and Is Related to the Apoptotic Response

Takashi Takano,[1,2,3] Michinori Kohara,[2] Yuri Kasama,[1] Tomohiro Nishimura,[1,4] Makoto Saito,[1] Chieko Kai,[3] and Kyoko Tsukiyama-Kohara[1]*

[1]*Faculty of Life Sciences, Department of Experimental Phylaxiology, Kumamoto University, Kumamoto, Japan*
[2]*Department of Microbiology and Cell Biology, Tokyo Metropolitan Institute of Medical Science, Tokyo, Japan*
[3]*Laboratory Animal Research Center, Institute of Medical Science, The University of Tokyo, Tokyo, Japan*
[4]*The Chemo-Sero-Therapeutic Research Institute, Kikuchi Research Center, Kyokushi, Kikuchi, Kumamoto, Japan*

The localization of hepatitis C virus (HCV) proteins in cells leads to several problems. The translocase of outer mitochondrial membrane 70 (TOM70) is a mitochondrial import receptor. In this study, TOM70 expression was induced by HCV infection. TOM70 overexpression induced resistance to tumor necrosis factor-alpha (TNF-α)-mediated apoptosis but not to Fas-induced apoptosis in HepG2 cells. TOM70 was found to be induced by the HCV non-structural protein (NS)3/4A protein, and silencing of TOM70 decreased the levels of the NS3 and Mcl-1 proteins. These results indicate that TOM70 can directly interact with the NS3 protein. In hepatoma cells, silencing of TOM70 induced apoptosis and increased caspase-3/7 activity but did not modify caspase-8 and caspase-9 activity. TOM70 silencing-induced apoptosis was impaired in HCV NS3/4A protein-expressing cells. Thus, this study revealed a novel finding, that is, TOM70 is linked with the NS3 protein and the apoptotic response. ***J. Med. Virol. 83:801–809, 2011.***

KEY WORDS: hepatitis C virus; translocase of outer mitochondrial membrane 70; apoptosis; non-structural protein 3; tumor necrosis factor-alpha

INTRODUCTION

Hepatitis C virus (HCV) infection causes acute and chronic hepatitis, cirrhosis, and hepatocellular carcinoma (HCC) [Seeff, 2002]. HCV easily establishes chronic infection, and localization of HCV proteins is reported to induce several disturbances in cells. One of the major target organelles of HCV is the mitochondrion, and HCV non-structural protein (NS)3/4A protease cleaves the mitochondrial antiviral signaling (MAVS)/IPS-1/VISA/Cardif protein, thereby impairing interferon signaling [Li et al., 2005] and influencing apoptotic responses [Nomura-Takigawa et al., 2006; Deng et al., 2008; Lei et al., 2009].

Most mitochondrial proteins are synthesized in the cytosol as preproteins, targeted to the mitochondria by cytosolic factors such as HSP70 and mitochondrial import stimulation factor (MSF), and transported to the intramitochondrial compartments by the preprotein import machineries of the outer and inner membranes (TOM and TIM complexes, respectively) [Mihara and Omura, 1996; Schatz, 1996; Neupert, 1997; Pfanner and Meijer, 1997]. The TOM machinery consists of two import receptors, namely, TOM20 and TOM70, and several other subunits that are arranged in a tightly bound complex termed the general import pore [Pfanner and Geissler, 2001; Hoogenraad et al., 2002; Stojanovski et al., 2003]. TOM70 was identified in *Saccharomyces cerevisiae* as a 70-kDa protein with no known function [Truscott et al., 2001]. TOM70 is recognized as the primary receptor for proteins with internal targeting signals, such as the F_1-ATPase β-subunit and cytochrome c_1 [Truscott et al., 2001]. TOM70 interacts with human myeloid cell leukemia-1 (Mcl-1), a Bcl-2 family member, and this interaction facilitates the mitochondrial targeting of Mcl-1 [Chou et al., 2006]. Mcl-1 can interact with the HCV core protein and suppresses core-induced apoptosis [Mohd-Ismail et al., 2009].

In the present study, it was found that TOM70 activity was enhanced by HCV. This study addresses TOM70 modification by HCV and its role in the apoptotic response.

Additional Supporting Information may be found in the online version of this article.

Grant sponsor: Ministry of Health and Welfare of Japan; Grant sponsor: Clinical and Epidemiological Studies of Emerging and Re-emerging Infectious Diseases (Cooperative Research Project).

Takashi Takano present address is Division of Veterinary Public Health, Nippon Veterinary and Life Science University, 1-7-1 Kyonan, Musashino, Tokyo 180-8602, Japan.

*Correspondence to: Kyoko Tsukiyama-Kohara, Faculty of Life Sciences, Department of Experimental Phylaxiology, Kumamoto University, 1-1-1 Honjo, Kumamoto 860-8556, Japan.
E-mail: kkohara@kumamoto-u.ac.jp

Accepted 13 December 2010
DOI 10.1002/jmv.22046
Published online in Wiley Online Library (wileyonlinelibrary.com).

MATERIALS AND METHODS

Cells

WRL68, HepG2, HuH-7, and HepG2 cells expressing non-structural proteins (Lenti-NS3/4A-HepG2, Lenti-NS4B-HepG2, Lenti-NS5A-HepG2, Lenti-NS5B-HepG2, and Lenti-empty-HepG2) were maintained and established as described previously [Tsukiyama-Kohara et al., 2004; Nishimura et al., 2009; Saitou et al., 2009]. The Cre/loxP conditional expression system for full-length HCV cDNA (*HCR6-Rz*) in RzM6 cells [Tsukiyama-Kohara et al., 2004] was induced using 100 nM of 4-hydroxytamoxifen (Sigma–Aldrich, St. Louis, MO) and passaged for 8 days (RzM6-8d) or for more than 44 days (RzM6-LC) [Nishimura et al., 2009] (Supplementary Fig. 1). Cell viability was measured using WST-8 (Dojindo, Kumamoto, Japan).

Purification and Matrix-Assisted Laser Desorption Ionization Time-of-Flight Mass Spectrometry (MALDI-TOF-MS) Analysis of p70 and TOM70 Expression Vector

p70 was identified using MALDI-TOF-MS. The p70 band was excised, alkylated using 40 mM iodoacetamide/0.1 M NH_4HCO_3, and digested using trypsin. The p70 peptides were purified using an UltiMate capillary high-performance liquid chromatography system (Dionex) and analyzed using a 4700 Proteomics Analyzer (Applied Biosystems, Foster City, CA), as described previously [Jensen et al., 1999]. An expression vector with myc and His tags was constructed for TOM70 as follows: Total RNA was isolated from HuH-7 cells (10^6) by using the ISOGEN reagent (Nippon Gene, Tokyo, Japan). Purified RNA (2 μg) was reverse transcribed using SuperScriptIII (Invitrogen, Carlsbad, CA) and oligo$(dT)_{12-18}$ primer (Invitrogen), according to the manufacturer's protocol. The coding region of TOM70 cDNA was amplified by polymerase chain reaction (PCR) with LA *Taq* polymerase (Takara Bio, Shiga, Japan) and TOM70-F2 (5′-GGATCCGCAGAGGACACTTGTCATGGC-3′), which contained a *Bam*HI restriction site (underlined), as the forward primer and TOM70-R2 (5′-GCTGGAGTGCAGTGGCTATTC-3′) as the reverse primer. The amplified TOM70 cDNA was subcloned into the pCR2.1-TOPO vector. *Bam*HI–*Eco*RI-digested TOM70 cDNA was subcloned into pcDNA6/Myc-His(+) (Invitrogen) (TOM70-pcDNA6).

Immunoprecipitation (IP) and Western Blotting (WB)

The cells were solubilized in lysis buffer (20 mM HEPES-NaOH [pH 7.5], 1 mM EDTA [pH 7.5], 1 mM dithiothreitol, 1 μM diisopropylfluorophosphate, 150 mM NaCl, and 1% TritonX-100). Samples were centrifuged at 20,400*g* for 10 min at 4°C, and the supernatants were used for IP. Protein-G sepharose 4B beads (GE Healthcare, Piscataway, NJ; 20 μl) were washed, mixed with 2-243a antibody (2 μg) in 1% BSA-phosphate-buffered saline (PBS), and placed on a rotary shaker at 4°C for 1 hr. Next, the beads were washed three times with lysis buffer and treated with the cell lysate (4°C, overnight). The IP mix was washed four times with lysis buffer and solubilized with 2× SDS sample buffer (150 mM Tris [pH 6.8], 4% SDS, 20% glycerol, 10% 2-mercaptoethanol, and 0.2% bromophenol blue). WB was performed as described previously [Nishimura et al., 2009]. Anti-myc monoclonal antibody (mAb) (9E10; Santa Cruz Biotechnology, Santa Cruz, CA), anti-HCV core mouse mAb (31-2), and anti-NS3 rabbit polyclonal antibody (R212) were used to examine the interaction between NS3 and myc-TOM70. Anti-Mcl-1 antibody (S-19; Santa Cruz Biotechnology) and anti-MAVS antibody (ab25084; ChIP grade; Abcam, Cambridge, MA) were also used. Professor Mihara (Kyusyu University) kindly provided anti-rat TOM70 polyclonal antibody (rTOM70).

Immunofluorescence Assay (IFA)

For mitochondrial staining, MitoRed (Dojindo) was added to the cell culture medium and incubated for 1 hr. The cells were fixed in 4% paraformaldehyde. The slides were then washed with PBS, permeabilized with 1% Triton X-100; and reacted with 2-243a mAb (1 μg/ml) and a polyclonal antibody against the endoplasmic reticulum (ER) (anti-PDI; 1:1,000; Stressgen Bioreagent, Kampenhout, Belgium) in 0.025% Tween-20 PBS, followed by reaction with FITC-conjugated goat anti-mouse IgG mAb (1:1,000; Cappel Products, Portland, ME) and Alexa 568-conjugated goat anti-rabbit IgG $(Fab')_2$ fragment (Invitrogen) in 0.025% Tween-20 PBS. The slides were covered with Vector Shield (Vector Laboratories, Burlingame, CA) and observed under an Olympus Fluoview laser-scanning microscope (Olympus, Tokyo, Japan).

Evaluation of Cell Death by Assessing Fas or Tumor Necrosis Factor (TNF)-α

The cells were plated in a 96-well plate (10^4 cells/well; Becton Dickinson, Franklin Lake, NJ) and transfected with empty pcDNA6 or TOM70-pcDNA6 (40 ng/well) by using the Lipofectamine 2000 reagent (Invitrogen). After 48 hr, the cells were treated with anti-Fas

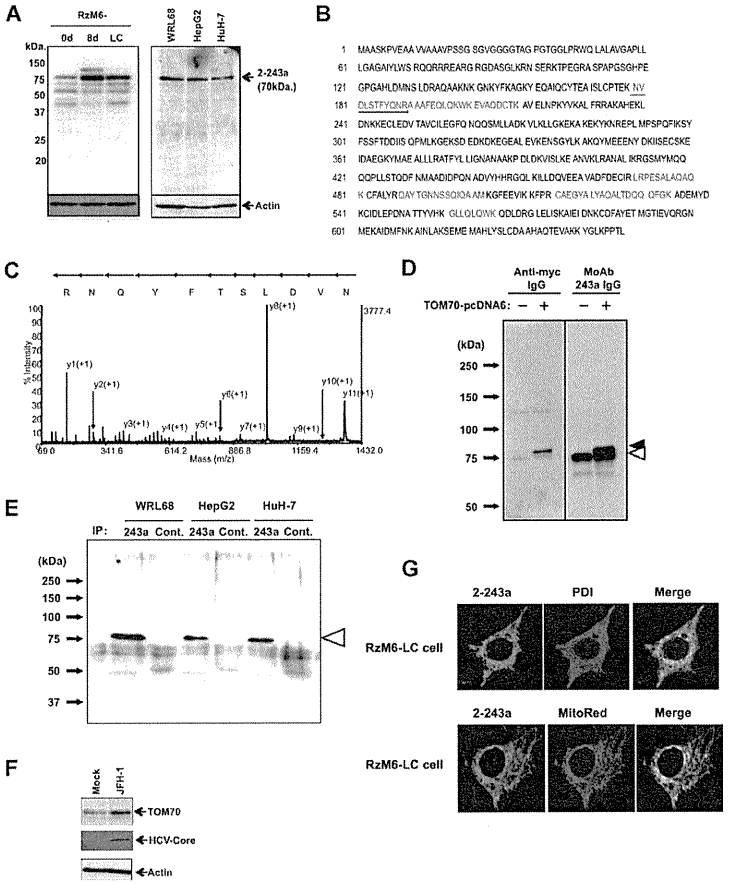

Fig. 1. TOM70 is induced by HCV and is localized in the mitochondria. **A**: TOM70 induction was examined by WB in RzM6-8d and RzM6-LC days (left panel), and TOM70 expression was compared in WRL68, HepG2, and HuH-7 cells (right panel). **B**: Identification of p70 by MALDI-TOF-MS analysis. The sequence of peptides in the amino acid sequence of TOM70 protein was determined using MALDI-TOF-MS analysis (red characters). **C**: MS/MS spectra of the peptide NVDLSTFYQNR (149–159). The sequence covers 14% of the amino acid sequence of TOM70. **D**: Identification of p70 by IP-WB. Expression of TOM70-pcDNA6 in HuH-7. Cell lysates were examined using WB with mAb 2-243a or the anti-myc antibody. myc-TOM70-pcDNA6 expression was recognized by both mAb 2-243a and the anti-myc antibody (black triangle). The expression of cellular TOM70 (empty triangle) was recognized only by mAb 2-243a. **E**: Cell lysates were immunoprecipitated with anti-rat TOM70 antibody and analyzed using WB with mAb 2-243a. The empty triangle indicates TOM70. The molecular weight markers are shown on the left. **F**: Expression of TOM70 and the core protein in mock- and HCV JFH-1-infected HuH-7 cells. **G**: Localization of TOM70 in RzM6-LC cells. The cells were stained with mAb 2-243a and polyclonal antibody against PDI or MitoRed. The magnification is 800×.

antibody (CH-11; 0–20 ng/ml; Beckman Coulter, Murmasaka) or recombinant human TNF-α (0–100 ng/ml; PeproTech, Rocky Hill, NJ), followed by addition of cycloheximide (CHX; 10 μg/ml). After treatment for 24 hr, apoptotic cell death was evaluated by determining cell viability with the WST-8 reagent. Next, the terminal deoxynucleotidyl transferase dUTP nick-end labeling (TUNEL) assay was performed using the TMR red in situ cell death detection kit (Roche, Basel, Switzerland).

Generation of Small Interfering Ribonucleic Acid (siRNA) for TOM70

siRNAs for two regions of TOM70, namely, TOM70-d1-siRNA (primer set: TOM70-dicer1-F and TOM70-dicer1-R) and TOM70-d2-siRNA (primer set: TOM70-dicer2-F and TOM70-dicer2-R) were generated.

Gene-specific dsDNA for TOM70 was constructed by PCR using TOM70-pcDNA6 as the template. TOM70-dicer1-F (5′-GCGTAATACGACTCACTATAGGGAGATGTTTGGCCTTTAAGTATCC-3′) was used as the forward primer, and TOM70-dicer1-R (5′-GCGTAATACGACTCACTATAGGGAGATGATATCATCCGTGAAAGAAC-3′) was used as the reverse primer; both primers contained a T7 promoter sequence (underlined). PCR performed using these primers yielded a 434-bp product. PCR with the forward primer TOM70-dicer2-F (5′-GCGTAATACGACTCACTATAGGGAGAATGTTTGCATTGTACCGCC-3′) and the reverse primer TOM70-dicer2-R2 (5′-GCGTAATACGACTCACTATAGGGAGATTTGCAACTTCTGTCTGGGC-3′), both of which contained a T7 promoter sequence (underlined), yielded a 474-bp product. Luciferase was amplified from pGL3-Basic (Takara Bio) with Luci-dicer2-F (5′-GCGTAATACGACTCACTATAGGGAGACGGTTTTGGAATGTTTACTAC-3′) as the forward primer and Luci-dicer2-R (5′-GCGTAATACGACTCACTATAGGGAGAGCTGATGTAGTCTCAGTGAGC-3′), as the reverse primer, yielding a 309-bp product; both primers contained a T7 promoter sequence (underlined). LA *Taq* polymerase was used for the PCR. All PCR products were analyzed by agarose electrophoresis before purification with the Wizard SV Gel and PCR Clean-Up System (Promega, Madison, WI).

In vitro transcription was performed with the Dicer siRNA generation kit (Genlantis, San Diego, CA), according to the manufacturer's instructions. Briefly, in vitro transcription reactions were performed in a 20-μl volume with 1 μg PCR product as the template; the reaction mixture was incubated at 37°C for 4 hr, followed by purification with the reagents provided in the Dicer siRNA generation kit. The dsDNA (20 μl) obtained was finally in a 100-μl volume after incubation at 37°C for 27 hr. The siRNAs obtained were purified and quantified according to the manufacturer's instructions.

Next, the cells were plated in 24- or 96-well plates (BD Bioscience, Sparks, MD) at a density of 5×10^4 or 10^4 cells/well, respectively, and left overnight for adherence. The siRNAs (14 nM) generated were transfected to cells by using Lipofectamine RNAiMAX (Invitrogen) and Opti-MEM (Invitrogen). The cells were characterized 48 hr after transfection.

Caspase Assay

The activities of caspase-3/7, caspase-8, and caspase-9 were measured on the basis of the cleavage of a proluminescent substrate containing the DEVD sequence, by using the commercially available Caspase-Glo 9 Assay, Caspase-Glo 8 Assay, and Caspase-Glo 3/7 Assay kits (Promega) and a luminometer (Aloka, Tokyo, Japan). Caspase activity was quantified according to the manufacturer's instructions.

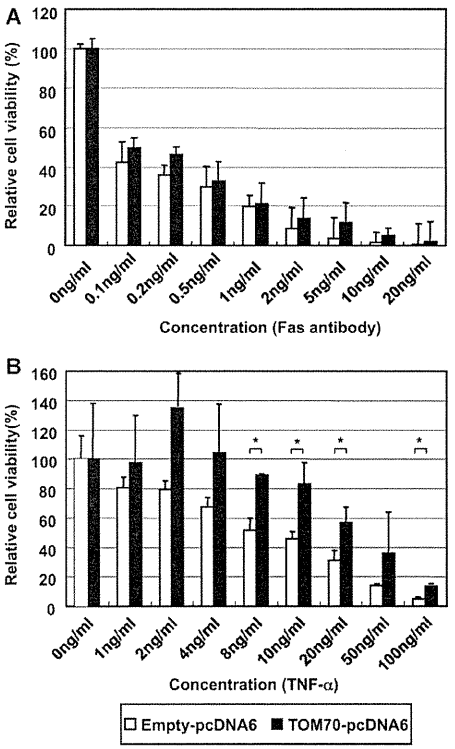

Fig. 2. TOM70 overexpression induced TNF-α-mediated apoptotic resistance. TOM70 overexpression affected TNF-α-mediated apoptosis but not Fas-mediated apoptosis. Cells were transfected with empty pcDNA6 (white bar) or TOM70-pcDNA6 (black bar). After 48 hr, they were treated with (**A**) Fas antibody (0–20 ng/ml) or (**B**) TNF-α (0–100 ng/ml). After 24 hr, cell viability was measured using WST-8. A,B: The data represent the average of the values obtained from triplicate experiments, and the vertical bars indicate the SD. $^*P < 0.05$ (two-tailed Student's *t*-test).

Statistical Analysis

Data were analyzed for statistical significance by using the Student's *t*-test. *P*-values lower than 0.05 were considered statistically significant.

RESULTS

Identification of the p70 Molecule and Induction by HCV

mAbs against RzM6-LC cells were screened, and the clone 2-243a, which recognizes p70, was obtained

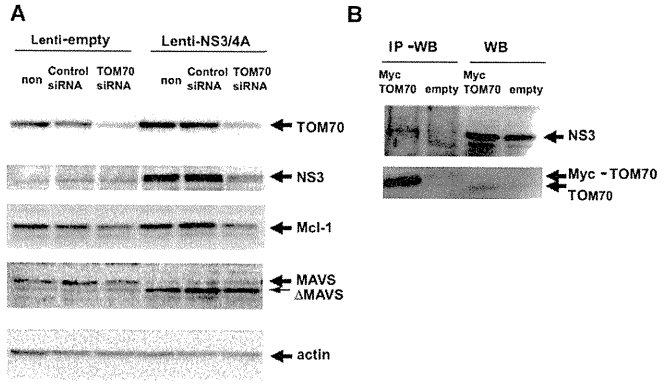

Fig. 3. Interaction between TOM70 and NS3 protein. **A**: The effect of TOM70 siRNA in cells transfected with empty or NS3/4A-containing lentivirus vectors was examined by WB with mAb 2-243a for TOM70; anti-NS3 rabbit polyclonal antibody; anti-Mcl-1 rabbit polyclonal antibody; anti-MAVS rabbit polyclonal antibody; and anti-actin antibody. **B**: The interaction between TOM70 and NS3 was assessed using IP-WB. NS3-expressing HepG2 cells were transfected with pcDNA6-TOM70 (mycTOM70) or pcDNA6 alone (empty) and immunoprecipitated with the anti-myc antibody (9E10). NS3 was detected using polyclonal rabbit anti-NS3 antibody (upper image), and TOM70 was detected using mAb 2-243a (lower image).

(Fig. 1A). p70 was induced to a greater extent by HCV expression after 8 days (RzM6-8d) or more than 44 days (RzM6-LC) than before HCV expression (RzM6-0d). The p70 expression level did not differ among the human hepatic cell lines (WRL68, HepG2, and HuH-7) (Fig. 1A, right panel). p70 was characterized (Fig. 1B–E): The sequence of peptides determined using MALDI-TOF-MS (Fig. 1B) and the MS/MS spectra of the p70 peptide sequence NVDLSTFYQNR (Fig. 1C) are provided. TOM70-pcDNA6 expression in HuH-7 cells was detected by WB with mAb 2-243a (Fig. 1D). Cell lysates were immunoprecipitated with anti-rat TOM70 antibody and detected by WB using mAb 2-243a (Fig. 1E). These results indicate that mAb 2-243a recognizes TOM70. Next, the effect of HCV infection on TOM70 expression was examined (Fig. 1F), and infection with the HCV JFH-1 strain [Wakita et al., 2005] induced TOM70 expression in HuH-7 cells (Fig. 1F). TOM70 localization was characterized using an indirect fluorescence assay (IFA) with 2-243a; anti-PDI, an ER marker; or MitoRed, which is a selective mitochondrial marker (Fig. 1G). TOM70 was associated with the mitochondria in all cells and was a part (~40%) of the ER, indicating that the TOM70 expressions in the mitochondria were higher than those in the ER.

TOM70 Inhibits TNF-α-Mediated Apoptotic Cell Death

The results of previous studies indicate the significant role of mitochondria in the apoptotic response [Hatano, 2007]. TOM70 interacts with Mcl-1 and facilitates mitochondrial targeting by the latter [Chou et al., 2006]. Mcl-1 silencing enhances TNF-related apoptosis-inducing ligand (TRAIL)-mediated cell death [Wirth et al., 2005; Han et al., 2006]. Therefore, the role of TOM70 in the apoptotic response was examined in this study. HepG2 cells were transfected with TOM70-pcDNA6 (Fig. 1D) or empty pcDNA6 (control), and their sensitivity to anti-Fas antibody (Fig. 2A) and TNF-α-mediated apoptotic cell death (Fig. 2B) was examined. When treated with 8 ng/ml of TNF-α, the TOM70-pcDNA6-transfected cells were significantly more viable than those transfected with empty pcDNA6 (Fig. 2B). In contrast, no significant differences were found between the viability of TOM70-pcDNA6 transfected cells and control cells treated with anti-Fas antibody (Fig. 2A). Thus, TNF-α-induced apoptosis was inhibited by TOM70 overexpression.

Interaction of TOM70 With HCV-NS3 and Other Host Factors

To determine the mechanism by which HCV induces TOM70, the TOM70 level in HCV NS3/4A-expressing HepG2 cells was determined (Fig. 3A). The TOM70 level was higher in the NS3/4A-expressing cells than in the control cells. Interestingly, the level of NS3/4A protein as well as Mcl-1 was reduced when TOM70 was silenced. The MAVS protein is cleaved by NS3/4A, as reported previously [Li et al., 2005], and the level of this protein was not influenced by the silencing of TOM70. IP-WB was performed to examine the possible interaction between TOM70 and NS3/4A (Fig. 3B). The pcDNA6-TOM70-myc plasmid was transfected into lenti-NS3/4A vector-transduced HepG2 cells; IP was performed using the anti-myc antibody, and the reaction was detected using the anti-NS3 antibody. The NS3 protein was

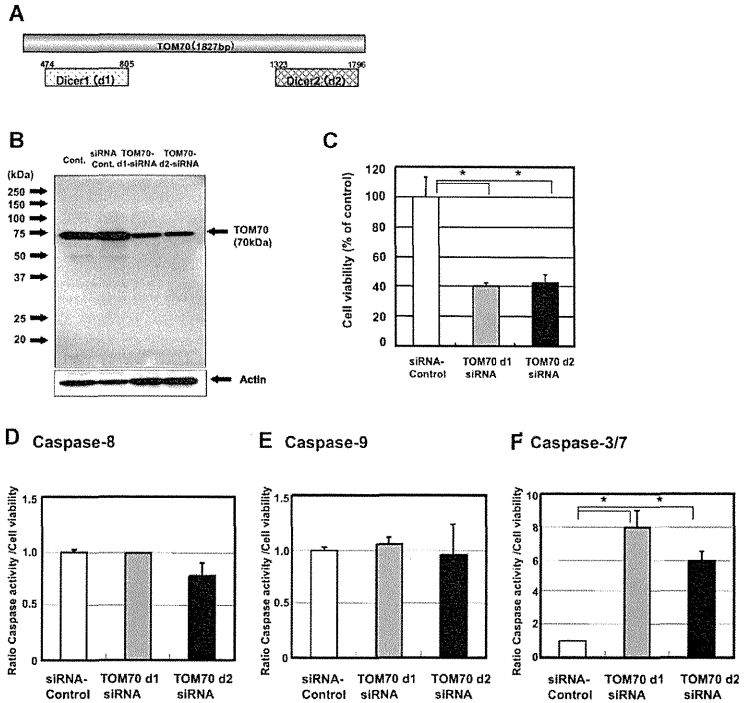

Fig. 4. Silencing of TOM70 induced apoptotic cell death and caspase-3/7 activity. **A**: The positions of TOM70-d1-siRNA and TOM70-d2-siRNA are indicated in the figure. **B**: siRNA-mediated silencing of TOM70 was detected by WB (Cont: no siRNA, siRNA Cont: siRNA control (Luci2-siRNA), TOM70-d1-siRNA, TOM70-d2-siRNA). **C**: TOM70 knockdown-induced cell death was calculated by measuring viability (%) with the WST-8 cell counting kit. The cell viability after 48 hr was scored in HepG2 cells transfected with the siRNA control Luci2-siRNA (□), TOM70-d1-siRNA (■), and TOM70-d2-siRNA (■). The activities of caspase-8 (**D**), caspase-9 (**E**), and caspase-3/7 (**F**) were measured using commercially available assays and a luminometer. The caspase activity was scored after 48 hr in TOM70-knockdown HepG2 cells transfected with control siRNA (□), TOM70-d1-siRNA (■), and TOM70-d2-siRNA (■). C–F: The data represent the average of the values obtained from triplicate experiments, and the vertical bars indicate the SD. $^*P < 0.05$ (two-tailed Student's *t*-test).

specifically precipitated by myc-tagged TOM70. The NS4A protein was not detected in this assay (data not shown). Therefore, the NS3 protein directly interacts with TOM70.

TOM70 Knockdown by RNAi Induces Apoptosis

The effect of TOM70 on the apoptotic response was examined because TOM70 silencing decreased the level of Mcl-1. First, two siRNAs for TOM70 (TOM70-d1-siRNA and TOM70-d2-siRNA) were designed in order to prevent the off-target effect (Fig. 4A). siRNA for luciferase (Luci-d2-siRNA) was used as a control (Fig. 4B). HepG2 cells were transfected with TOM70-d1-siRNA or TOM70-d2-siRNA, and the downregulation of TOM70 expression was confirmed by WB (Fig. 4B). Furthermore, decreased cell viability was observed (Fig. 4C) after 48 hr. Treatment with TOM70-d1-siRNA or TOM70-d2-siRNA significantly decreased the cell viability of HuH-7 cells too (data not shown). These results indicate that TOM70 silencing with siRNA may induce apoptosis.

The activities of caspase-3/7, caspase-8, and caspase-9 in HepG2 cells were examined after TOM70 silencing (Fig. 4D–F). The activities of caspase-8 and caspase-9 in cells transfected with TOM70 siRNA were not significantly different from those in the cells treated with control siRNA (Fig. 4D,E). In contrast, the caspase-3/7 activity in the TOM70-siRNA transfected cells was significantly greater than that in the cells treated with